Response of debris-covered glaciers in the Mount Everest region to recent warming, and implications for outburst flood hazards — **Source link** ⧉

Douglas I. Benn, Douglas I. Benn, Tobias Bolch, Tobias Bolch ...+10 more authors

Institutions: University of St Andrews, University Centre in Svalbard, University of Zurich, Dresden University of Technology ...+6 more institutions

Related papers:

- The state and fate of Himalayan glaciers

- Contrasting patterns of early twenty-first-century glacier mass change in the Himalayas

- Spatially variable response of Himalayan glaciers to climate change affected by debris cover

- Ice Melting under a Thin Layer of Moraine, and the Existence of Ice Cores in Moraine Ridges

- Region-wide glacier mass balances over the Pamir-Karakoram-Himalaya during 1999–2011

Response of debris-covered glaciers in the Mount Everest region to recent warming, and implications for outburst flood hazards
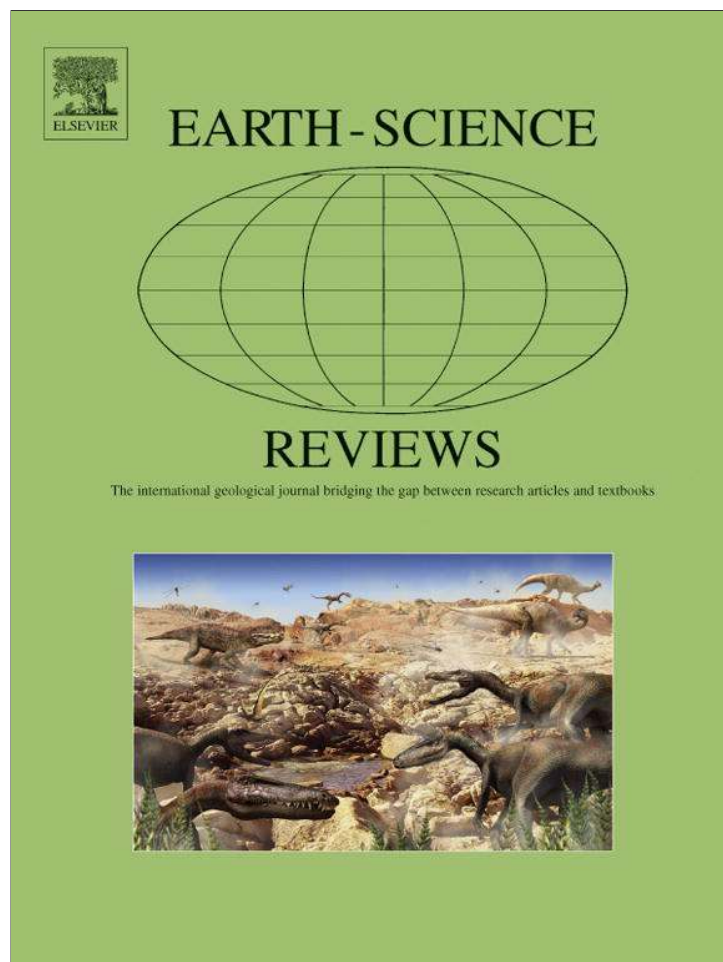
Benn, D I ; Bolch, Tobias ; Hands, K ; Gulley, J ; Luckman, A ; Nicholson, L I ; Quincey, D ; Thompson, S ; Toumi, R ; Wiseman, S

Abstract: In areas of high relief, many glaciers have extensive covers of supraglacial debris in their ablation zones, which alters both rates and spatial patterns of melting, with important consequences for glacier response to climate change. Wastage of debris-covered glaciers can be associated with the formation of large moraine-dammed lakes, posing risk of glacier lake outburst floods (GLOFs). In this paper, we use observations of glaciers in the Mount Everest region to present an integrated view of debris-covered glacier response to climate change, which helps provide a long-term perspective on evolving GLOF risks. In recent decades, debris-covered glaciers in the Everest region have been losing mass at a mean rate of 0.32 m yr [1], although in most cases there has been little or no change in terminus position. Mass loss occurs by 4 main processes: (1) melting of clean ice close to glacier ELAs; (2) melting beneath surface debris; (3) melting of ice cliffs and calving around the margins of supraglacial ponds; and (4) calving into deep proglacial lakes. Modelling of processes (1) and (2) shows that Everest-region glaciers typically have an inverted ablation gradient in their lower reaches, due to the effects of a down-glacier increase in debris thickness. Mass loss is therefore focused in the mid parts of glacier ablation zones, causing localised surface lowering and a reduction in downglacier surface gradient, which in turn reduce driving stress and glacier velocity, so the lower ablation zones of many glaciers are now stagnant. Model results also indicate that increased summer temperatures have raised the altitude of the rain–snow transition during the summer monsoon period, reducing snow accumulation and ice flux to lower elevations. As downwasting proceeds, formerly efficient supraglacial and englacial drainage networks are broken up, and supraglacial lakes form in hollows on the glacier surface. Ablation rates around supraglacial lakes are typically one or two orders of magnitude greater than sub-debris melt rates, so extensive lake formation accelerates overall rates of ice loss. Most supraglacial lakes are 'perched' above hydrological base level, and are susceptible to drainage if they become connected to the englacial drainage system. Speleological surveys of conduits show that large englacial voids can be created by drainage of warm lake waters along pre-existing weaknesses in the ice. Roof collapses can open these voids up to the surface, and commonly provide the nuclei of new lakes. Thus, by influencing both lake drainage and formation, englacial conduits exert a strong control on surface ablation rates. An important threshold is crossed when downwasting glacier surfaces intersect the hydrological base level of the glacier. Base-level lakes formed behind intact moraine dams can grow monotonically, and in some cases can pose serious GLOF hazards. Glacier termini can evolve in different ways in response to the same climatic forcing, so that potentially hazardous lakes will form in some situations but not others. Additionally, the probability of a flood is not simply a function of lake volume, but depends on the geometry and structure of the dam, and possible trigger mechanisms such as ice- or rockfalls into the lake. Satellite-based measurements of glacier surface gradient and ice velocities allow probable future locations of base-level lakes to be identified. A base-level lake has begun to grow rapidly on Ngozumpa Glacier west of Mount Everest, and could attain a volume of 10 m³ within the next 2 or 3 decades. Unless mitigation efforts are undertaken, this lake could pose considerable GLOF hazard potential.

EARTH-SCIENCE REVIEWS

The international geological journal bridging the gap between research articles and textbooks

(This is a sample cover image for this issue. The actual cover is not yet available at this time.)

Response of debris-covered glaciers in the Mount Everest region to recent warming, and implications for outburst flood hazards

D.I. Benn [a,b,*], T. Bolch [c,d], K. Hands [e], J. Gulley [a,f], A. Luckman [g], L.I. Nicholson [h], D. Quincey [i], S. Thompson [a,g], R. Toumi [j], S. Wiseman [k]

[a] The University Centre in Svalbard, P.O. Box 156, N-9170 Longyearbyen, Norway
[b] School of Geography and Geosciences, University of St. Andrews, Fife, KY16 9AL, UK
[c] Geographisches Institut, Universität Zürich, 8057 Zürich, Switzerland
[d] Institut für Kartographie, Technische Universität Dresden, 01069 Dresden, Germany
[e] URS/Scott Wilson, 23 Chester Street, Edinburgh, EH3 7EN, UK
[f] Institute for Geophysics, University of Texas, Austin, TX 78758–4445, USA
[g] Department of Geography, College of Science, Swansea University, SA2 8PP, UK
[h] Institute of Meteorology and Geophysics, Universität Innsbruck, 6020 Innsbruck, Austria
[i] School of Geography, University of Leeds, Leeds, LS2 9JT, UK
[j] Department of Physics, Imperial College, London SW72AZ, UK
[k] Department of Geography, University of Aberdeen, AB24 3UF, UK

ARTICLE INFO

ABSTRACT

In areas of high relief, many glaciers have extensive covers of supraglacial debris in their ablation zones, which alters both rates and spatial patterns of melting, with important consequences for glacier response to climate change. Wastage of debris-covered glaciers can be associated with the formation of large moraine-dammed lakes, posing risk of glacier lake outburst floods (GLOFs). In this paper, we use observations of glaciers in the Mount Everest region to present an integrated view of debris-covered glacier response to climate change, which helps provide a long-term perspective on evolving GLOF risks.

In recent decades, debris-covered glaciers in the Everest region have been losing mass at a mean rate of ~0.32 m yr^{-1}, although in most cases there has been little or no change in terminus position. Mass loss occurs by 4 main processes: (1) melting of clean ice close to glacier ELAs; (2) melting beneath surface debris; (3) melting of ice cliffs and calving around the margins of supraglacial ponds; and (4) calving into deep proglacial lakes. Modelling of processes (1) and (2) shows that Everest-region glaciers typically have an inverted ablation gradient in their lower reaches, due to the effects of a down-glacier increase in debris thickness. Mass loss is therefore focused in the mid parts of glacier ablation zones, causing localised surface lowering and a reduction in downglacier surface gradient, which in turn reduce driving stress and glacier velocity, so the lower ablation zones of many glaciers are now stagnant. Model results also indicate that increased summer temperatures have raised the altitude of the rain–snow transition during the summer monsoon period, reducing snow accumulation and ice flux to lower elevations.

As downwasting proceeds, formerly efficient supraglacial and englacial drainage networks are broken up, and supraglacial lakes form in hollows on the glacier surface. Ablation rates around supraglacial lakes are typically one or two orders of magnitude greater than sub-debris melt rates, so extensive lake formation accelerates overall rates of ice loss. Most supraglacial lakes are 'perched' above hydrological base level, and are susceptible to drainage if they become connected to the englacial drainage system. Speleological surveys of conduits show that large englacial voids can be created by drainage of warm lake waters along pre-existing weaknesses in the ice. Roof collapses can open these voids up to the surface, and commonly provide the nuclei of new lakes. Thus, by influencing both lake drainage and formation, englacial conduits exert a strong control on surface ablation rates.

An important threshold is crossed when downwasting glacier surfaces intersect the hydrological base level of the glacier. Base-level lakes formed behind intact moraine dams can grow monotonically, and in some cases can pose serious GLOF hazards. Glacier termini can evolve in different ways in response to the same climatic forcing, so that potentially hazardous lakes will form in some situations but not others. Additionally, the probability of a flood is not simply a function of lake volume, but depends on the geometry and structure of the dam, and possible trigger mechanisms such as ice- or rockfalls into the lake. Satellite-

* Corresponding author at: The University Centre in Svalbard, P.O. Box 156, N-9170 Longyearbyen, Norway. Tel.: +47 79 02 3367.
E-mail address: doug.benn@unis.no (D.I. Benn).

based measurements of glacier surface gradient and ice velocities allow probable future locations of base-level lakes to be identified. A base-level lake has begun to grow rapidly on Ngozumpa Glacier west of Mount Everest, and could attain a volume of ~10^8 m^3 within the next 2 or 3 decades. Unless mitigation efforts are undertaken, this lake could pose considerable GLOF hazard potential.

Contents

1. Introduction

Debris cover affects glacier response to climate change by altering surface ablation rates and spatial patterns of mass loss (Nakawo et al., 1999; Benn and Lehmkuhl, 2000; Kirkbride, 2000; Benn et al., 2003). In high-relief mountain regions such as the Himalaya, debris-covered glaciers are widespread, influencing regional-scale patterns of glacier length change, mass balance and ice dynamics (Bolch et al., 2008a, 2008b; Quincey et al., 2009; Scherler et al., 2011). Although the Himalaya are expected to contribute relatively little to 21st century sea-level rise (Radić and Hock, 2011), glacier mass loss can be expected to have significant impacts at the catchment scale, including long-term reduction of water resources and increased frequency of glacier lake outburst floods (GLOFs). Glacier recession can lead to increased probability of GLOF events where large lakes develop behind weak moraine dams (Yamada, 1998; Richardson and Reynolds, 2000). In recent years, several well-documented outburst flood events have caused loss of life, dwellings, infrastructure and farmland (e.g. Vuichard and Zimmermann, 1987; Kattelmann, 2003; Fujita et al., 2009). The destructiveness of these events has motivated several studies of extant moraine-dammed lakes, and the development of criteria for hazard assessment (e.g. Reynolds, 2000; Bajracharya and Mool, 2009; Quincey et al., 2007; Bolch et al., 2008a, 2011a; Huggel et al., 2004).

Mass loss and lake formation on debris-covered glaciers are outcomes of a cascade of processes that translate climatic signals into changes in glacier ablation zones. The presence of an extensive debris cover means that the chain of cause and effect is considerably more complex than on debris-free glaciers, with the consequence that glacier response to climate forcing may be strongly non-linear. Depending on initial conditions, glacier termini can evolve in different ways in response to the same climatic forcing, so that potentially hazardous lakes will form in some situations but not others. To assess possible future changes in runoff and GLOF hazards in a catchment, therefore, it is important to consider the glaciological context, particularly the controls on mass balance, ice dynamics, and meltwater evacuation and storage.

This paper draws upon a broad range of field and remote-sensing observations in the Mount Everest region to present an integrated view of debris-covered glacier response to climate change. To include as large a sample of glaciers as possible, we define the Everest region broadly, to include the entire horseshoe-shaped complex of peaks and ridges straddling the border between Nepal and Tibet (China), between the Tama Kosi basin in the west, the Dudh Kosi basin in the south, and the Arun river basin in the north and east (Fig. 1). This complex massif includes four of the six highest mountains in the world: Mount Everest (Qomolungma, Sagarmatha: 8848 m), Lhotse (8516 m), Makalu (8462 m) and Cho Oyu (8201 m), as well as numerous peaks over 7000 m.

We begin with a discussion of climate and climate change in the region, and an overview of the characteristics of its debris-covered glaciers. We then summarise knowledge of recent glacier elevation changes and rates of ice flow, as determined from remote sensing data. There is a complete lack of in-situ mass balance data for debris-covered glaciers in the Everest region, and we address this data gap using a new model, which calculates theoretical mass-balance gradients from debris thickness and meteorological data. We then turn to the role of ephemeral supraglacial lakes in glacier ablation, and examine the controls on lake formation, growth and drainage. To a large degree, the life cycle of ephemeral lakes is controlled by subsurface drainage systems, and we discuss the origin and evolution of these systems using data from speleological surveys. On some glaciers, mass loss leads to the formation of moraine-dammed lakes, which can then grow to sufficient size to present significant GLOF hazards. We review processes and patterns of lake evolution, using selected case studies to illustrate the controls on lake inception, growth and drainage. We conclude by presenting a summary conceptual model of the evolution of Himalayan debris-covered glaciers during periods of negative mass balance, emphasising the links between different components of the system and the implications for predicting future glacier mass loss and hazard potential.

2. Climatic background

The Mount Everest region is near the northern limit of the South Asian monsoon, and experiences a summer precipitation maximum and cold, drier winters. Data from the Pyramid Meteorological Station
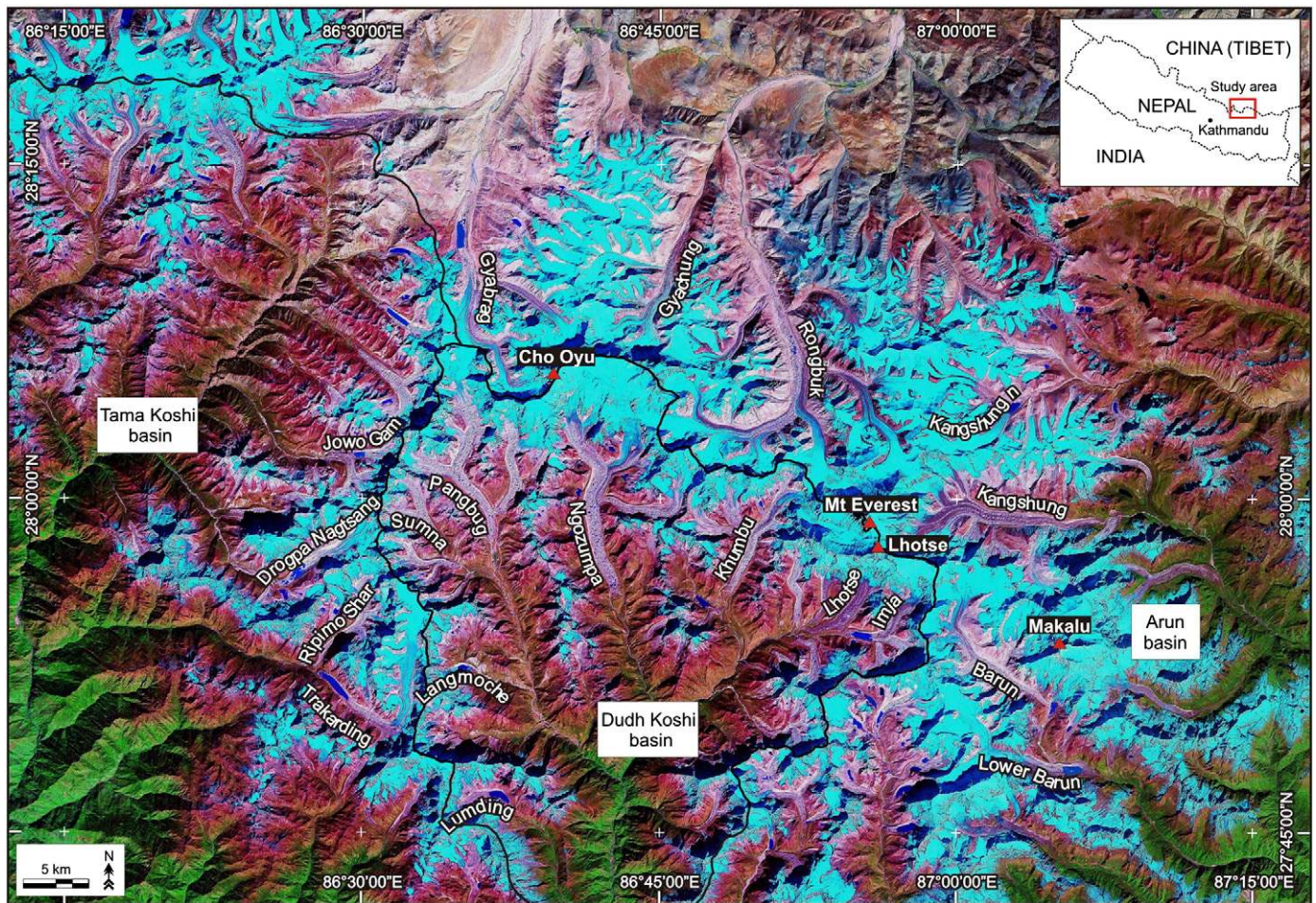
Fig. 1. Landsat image of the Everest region, showing the location of glaciers mentioned in the text.

near Lobuche on the western side of Khumbu Glacier (5050 m) show that 85% of the annual precipitation falls in the months of June to September (Fig. 2; Bertolani et al., 2000). Heavy autumn and winter snowfalls can occur in association with tropical cyclones and westerly disturbances, respectively, and snow accumulation can occur at high elevations at all times of the year. Data compiled by Asahi (2010) show a pronounced reduction in precipitation from south to north up the Dudh Kosi valley to the south of Mount Everest. Annual precipitation totals exceed 2 m yr^{-1} at 2000 m a.s.l. near the mountain front, and decline to 465 mm yr^{-1} adjacent to Khumbu

Fig. 2. Monthly mean temperature and precipitation data, Pyramid Weather Station, 5050 m (1994–1998). (Data from Bertolani et al., 2000).

Glacier (~5000 m above sea level). At Tingri to the north of Mount Everest, precipitation is only 296 mm yr^{-1} (Yang et al., 2006). Orographic effects superimpose significant local variation upon this broad regional gradient (Barros et al., 2004). Summer precipitation totals on peaks and ridges (5000–5500 m a.s.l.) in the Khumbu and Shorong Himal can be 4 to 5 times those in the adjacent valley (Yasunari and Inoue, 1978). Direct measurements of precipitation from elevations over 5000 m are almost completely lacking, although in recent years this data gap has been addressed using satellite data, particularly the Precipitation Radar aboard the Tropical Rainfall Measuring Mission (TRMM: e.g. Bhatt and Nakamura, 2005; Bookhagen and Burbank, 2006; Yamamoto et al., 2011). However, inconsistencies exist between different remote sensing data products, and estimation of precipitation totals at high elevations remains challenging (Andermann et al., 2011).

Climatic records in the Himalaya tend to be of short duration, limiting our ability to detect and quantify climate change. Shrestha et al. (1999) presented evidence for a warming trend (based on monthly means of daily maximum temperature) in the Nepal Himalaya, with an increase of ~0.6 °C per decade between 1971 and 1994, and Shrestha and Aryal (2011) reported that warming has continued since that time. The highest station in the vicinity of Mount Everest used in their study was at only 2770 m, and it is not known whether a similar warming trend has also been experienced at higher elevations. However, data from Tingri, at 4300 m on the north side of Everest also show a warming trend, of ~0.3 °C per decade (Yang et al., 2006). Climatic records reveal little or no trend in precipitation on either the Nepalese or Chinese side of Mount Everest, although there is large internal and inter-decadal variation associated with large-scale
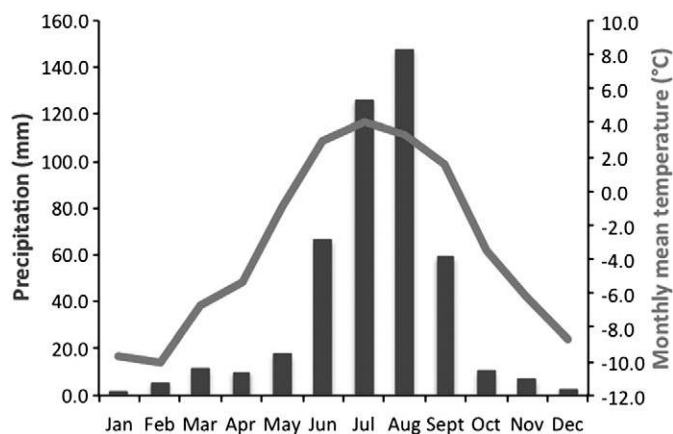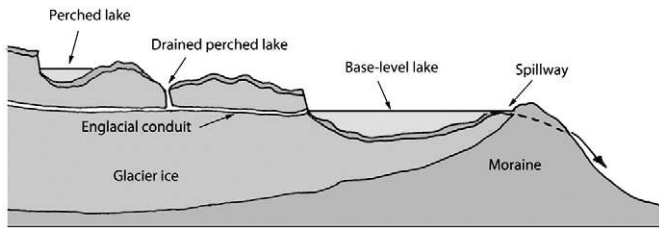
Fig. 3. Schematic diagram showing definition of perched and base-level lakes.

phenomena such as ENSO (Shrestha et al., 2000; Yang et al., 2006; Shrestha and Aryal, 2011).

3. Glaciers of the Everest region

The Everest region, as defined here, contains an area of 1930 km^2 of glacier ice and permanent snow, of which 445 km^2 is debris-covered ice (Fig. 1). The published glacier inventory for the Dudh Kosi drainage basin on the south side of Mount Everest (Higuchi et al., 1980, 2010) lists 664 glaciers. Only 47 of these glaciers are debris-covered although they occupy approximately 80% of the total glacierised area (Fushimi et al., 1980; Sakai et al., 2000b). The total volume of glacier ice in the Everest region is not known. Systematic ice thickness measurements have only been made on Khumbu Glacier (Gades et al., 2000), indicating that maximum measured ice thickness decreases from ~440 m at 0.5 km below the Khumbu Icefall to less than 20 m at 2 km from the terminus. Average ice thickness in the ablation zone is 125 m.

Three major debris-covered glaciers flow from the flanks of Mount Everest: Khumbu Glacier to the south, Rongbuk Glacier to the north, and Kangshung Glacier to the east. Other major debris-covered glaciers in the region include the 18 km long Ngozumpa Glacier on the south side of Cho Oyu (the longest glacier in the Everest region), Lhotse and Imja-Lhotse Shar Glaciers south of Mount Everest, Gyabrag and Gyachung Glaciers north of Cho Oyu, Barun Glacier south of Makalu, and Trakarding Glacier in the south-west (Fig. 1). In addition, there are large numbers of small glacier-like features with active frontal
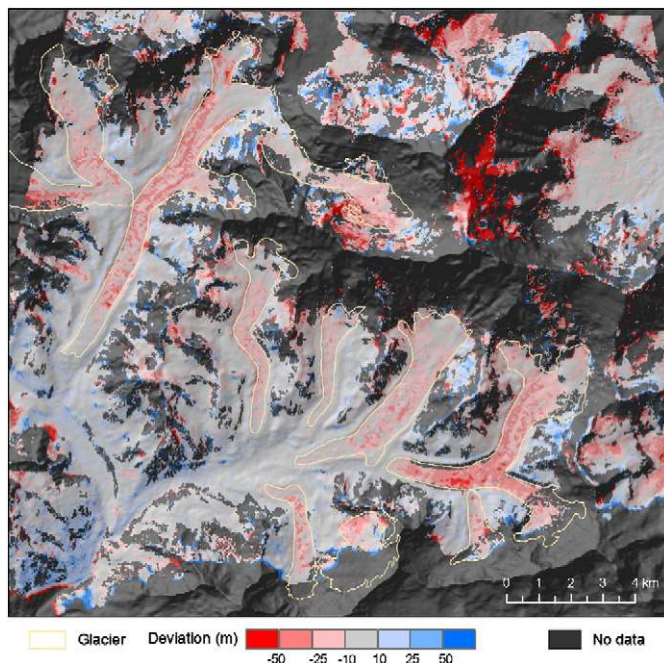

Fig. 4. Glacier elevation changes in the Khumbu region, 1970–2007. (From Bolch et al., 2011a).
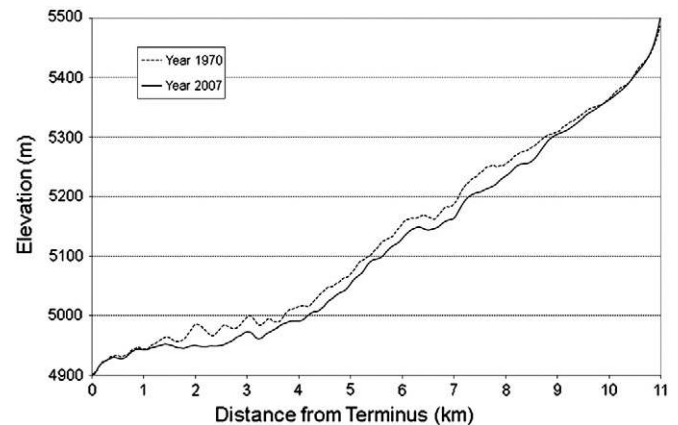

Fig. 5. Longitudinal surface elevation profiles of Khumbu Glacier, 1970 (solid line) and 2007 (dashed line). (From Bolch et al., 2011a).

slopes of boulders. The lower limit of these features at or slightly below the limit of permafrost (which was measured to be between 5400 and 5500 m in southern aspects, Fukui et al., 2007) indicates that these are bodies of permafrost creep ("rock glaciers") as described by Jakob (1992) and Barsch and Jakob (1998). However, the difference between rock glaciers and debris-covered glaciers may be to some extent arbitrary and more work is needed to clarify their characteristics and relationships in the study region.

Glacier equilibrium-line altitudes (ELAs) in the Dudh Kosi basin have been estimated by Asahi (2010), and rise from ~5200 m in the south to ~5700 m near the Nepal–Tibet border. Best estimates of glacier ELAs on the north side of Mount Everest are in the range ~5900 to 6300 m (Mann et al., 1996; Owen et al., 2009). The general northward rise of ELAs in the region is attributed to the precipitation gradient, reflecting the diminishing influence of the South Asian monsoon (Asahi, 2010). It should be emphasised, however, that little systematic work has been done on quantifying glacier ELAs in the Himalaya, and large uncertainties remain about their spatial variation and temporal trends (cf. Fujita and Nuimura, 2011).

Debris-covered glaciers in the region are typically overlooked by precipitous mountainsides, from which avalanches deliver snow, ice and rock onto the glacier surfaces (Benn and Owen, 2002; Hambrey et al., 2008). Some of the larger glaciers also have snowfields in their upper parts, where accumulation occurs by direct snowfall (e.g. the Western Cwm at the head of Khumbu Glacier). Many glaciers, however, lack snowfields, and all accumulation occurs in avalanche cones at the base of steep backwalls (Benn and Lehmkuhl, 2000). Because glacier ice originating from avalanches is generally heavily freighted with rock debris, a debris cover tends to develop immediately below the ELA of avalanche-fed glaciers. In contrast, glaciers with snowfields as well as avalanche-accumulation areas can have extensive clean-ice areas between their ELAs and areas of debris melt-out. This fact is important to consider when attempting to estimate ELAs from the maximum elevation of debris cover (Owen et al., 2009).

The lithological composition of debris cover reflects that of the source outcrops, and glaciers in catchments with complex geology can exhibit compositional 'striping', which can influence glacier albedo and energy balance (Fushimi et al., 1980; Casey et al., 2012). Values of debris albedo measured on Ngozumpa Glacier by Nicholson (2005) were mainly in the range 0.15 to 0.25, with a few higher outliers associated with concentrations of leucogranite boulders. There have been few systematic measurements of debris thicknesses on Everest-region glaciers. Nakawo et al. (1986) and Watanabe et al. (1986) reported debris thickness measurements made at ~50 sites on Khumbu Glacier. Debris emerges on the glacier surface near Everest Base Camp at 5300 m (~400 m below the ELA),

from where it increases to ~2.5 m in thickness near the glacier terminus. Measurements made on Ngozumpa Glacier by Nicholson (2005) also show an overall downglacier increase in debris thickness, but with considerable variability at each site.

Most debris-covered glaciers in the region are flanked by large lateral and terminal moraines, formed by reworking of supraglacial debris by gravitational and glacifluvial processes (Benn and Owen, 2002; Hambrey et al., 2008). Some moraines are known to have accumulated in multiple episodes spanning the entire Holocene period (Richards et al., 2000), and the largest examples are several hundreds of metres across and ~200 m high.

Most debris-covered glaciers in the Everest region have undergone significant downwasting in recent decades (Bolch et al., 2008b, 2011a). Downwasting has been accompanied by a reduction in glacier surface gradients and velocities, and large parts of the lower ablation zones of the major glaciers are now stagnant (Seko et al., 1998; Luckman et al., 2007; Bolch et al., 2008a; Quincey et al., 2009). The tongues of the large debris-covered glaciers are typically highly irregular and studded with supraglacial ponds and lakes. Benn et al. (2001) recognised a fundamental distinction between two types of supraglacial lakes, based on their elevation relative to the base level of the glacial hydrological system (Fig. 3). *Perched lakes* are located above the level at which water leaves the glacier. Some terminal moraines allow subsurface water flow (Hambrey et al., 2008) but the majority appear to form essentially impermeable barriers and all water leaving the glaciers flows via low points on the crest. In such cases, the lowest point on the moraine determines the hydrological base level for the glacier. Perched lakes can persist only if they are underlain by impermeable glacier ice, and rarely exceed 100 to 200 m in diameter before drainage occurs (Benn et al., 2001). In contrast, *base-level lakes* are located at the elevation at which water leaves the glacier. Such lakes will persist so long as the moraine dam remains intact, and have the potential to develop into large, moraine-dammed lakes. Drainage of base-level lakes can be gradual or catastrophic, depending on the geometry and composition of the moraine dam and other factors (Richardson and Reynolds, 2000).

Several glacier lake outburst floods (GLOFs) have occurred in the Everest region in recent decades (Kattelmann, 2003; Bajracharya and Mool, 2009). In 1977, drainage of a series of lakes on and below Nare Glacier, south of Ama Dablam, caused significant erosion and loss of agricultural land downstream (Buchroithner et al., 1982). A more serious event occurred in 1985, when Dig Tsho, a moraine-dammed lake in front of Langmoche Glacier, almost completely drained following an ice avalanche (Vuichard and Zimmermann, 1987). Peak discharge was around 2000 m³ s⁻¹, and the flood destroyed a newly completed hydro-electric plant, numerous homes and several hectares of agricultural land, and caused at least 4 fatalities. Another event occurred in September 1998, when Sabai Tsho burst through its moraine barrier following a slope failure into the lake (Osti et al., 2011). These events brought the risk of GLOFs in the region to the attention of local people and the scientific and development communities, and highlighted the need for hazard assessment and remediation (Reynolds, 1998; Yamada, 1998). In addition to these well-documented events, several GLOFs have also occurred in more remote parts of the region. For example, in 1991 an outburst occurred at Ripimo Shar Glacier in the Tama Koshi catchment (Yamada and Sharma, 1993), and erosional scars indicate that there have been additional events unrecorded in the scientific literature.

4. Recent changes in glacier volume

Bolch et al. (2008b, 2011a) measured volume changes on a sample of glaciers south of Mount Everest, using Digital Elevation Models (DEMs) derived from Corona, ASTER and Cartosat-1 satellite data, and vertical aerial photographs taken by Swissair in 1984. These data were used to calculate glacier-wide volume losses, expressed as a water-equivalent mean rate of surface lowering. All 10 glaciers in the sample underwent net thinning during the study period (1970–2007), with a mean lowering rate of -0.32 ± 0.08 m yr⁻¹ (Fig. 4). For the period 2001–2007, the mean rate of change was -0.79 ± 0.52 m yr⁻¹, about double the longer-term rate of loss, although the uncertainty for the later period is high and the apparent accelerated volume loss is not statistically significant.

For the period 1970–2007, the highest mean lowering rate was on Imja–Lhotse Shar Glacier, which calves into a moraine-dammed base-level lake (0.50 ± 0.09 m yr⁻¹). This is substantially higher than the other glaciers in the sample, which experienced mean lowering rates in the range from -0.18 ± 0.07 to -0.30 ± 0.08 m yr⁻¹. The high mass loss is only partly attributable to calving losses at the glacier terminus, and large areas of the glacier surface also experienced high rates of surface lowering. Satellite thermal data and exposures in ice cliffs indicate that debris cover is relatively thin on this glacier, which may lead to higher than average melt rates (Suzuki et al., 2007; Bolch et al., 2011a).

DEM differencing also reveals substantial within-glacier variations in elevation change. On most of the glaciers, the maximum amount of mass loss is not close to the terminus, as would be expected on clean-ice glaciers, but is further up the ablation area. On Khumbu Glacier, rates of surface lowering are very small within 2 km of terminus, whereas between 2 and 8 km from the terminus, average lowering rates are around 0.6 m yr⁻¹ (1970–2007). This has resulted in a reduction of glacier gradient in the lowermost few km (Fig. 5). In addition, on most glaciers there are localised areas of high mass loss, associated with supraglacial ponds or meltwater channels.

Elevation change at a particular locality on a glacier surface reflects both surface mass balance and dynamic thickness changes resulting from ice flow, as expressed in the mass continuity equation:

$$\frac{\partial h}{\partial t} = \dot{b} + h\dot{\varepsilon}_{zz} - \bar{U}.\nabla h \tag{1}$$

where h is ice thickness, t is time, $\dot{b}$ is the surface balance rate, $\bar{U}$ is the vertically averaged ice velocity and $\dot{\varepsilon}_{zz}$ is the normal strain rate in the vertical (z) direction. The vertical normal strain rate reflects horizontal divergence (assuming incompressibility), such that thinning results from extending flow and vice versa. On stagnant parts of the glaciers, $\bar{U}$ and $\dot{\varepsilon}_{zz}$ are zero, so rates of elevation change equal the local balance rate. In areas of active ice flow, the balance rate cannot be disentangled from dynamic factors without knowledge of both ice thickness and the velocity field. Combined velocity and thickness data are available for only one glacier (Khumbu Glacier: Gades et al., 2000; Bolch et al., 2008b; Quincey et al., 2009), although coverage is incomplete. Nuimura et al. (2011) conducted a mass-continuity analysis of part of Khumbu Glacier, and found that the area below the icefall had undergone little net elevation change, apparently due to the opposing effects of reduced ice flux from the accumulation zone and less negative mass balance. Insufficient data are available for glacier-wide analyses, but in the following sections we use measurements of ice velocity together with theoretical considerations to identify the main controls on the observed patterns of elevation change.

5. Ice velocities

Point velocity measurements have been made on glaciers in the Everest region at various times since the 1950s, particularly on Khumbu Glacier (e.g. Kodama and Mae, 1976; Seko et al., 1998). With the development of automated feature tracking and interferometric remote sensing techniques, comprehensive velocity data have now been obtained for several glaciers in the region, allowing glacier-wide and regional patterns to be determined (Luckman et al., 2007; Bolch et al., 2008a; Scherler et al., 2008; Quincey et al., 2009).

Quincey et al. (2009) recognised three types of velocity structure on debris-covered glaciers in the Everest region (Fig. 6). Type 1
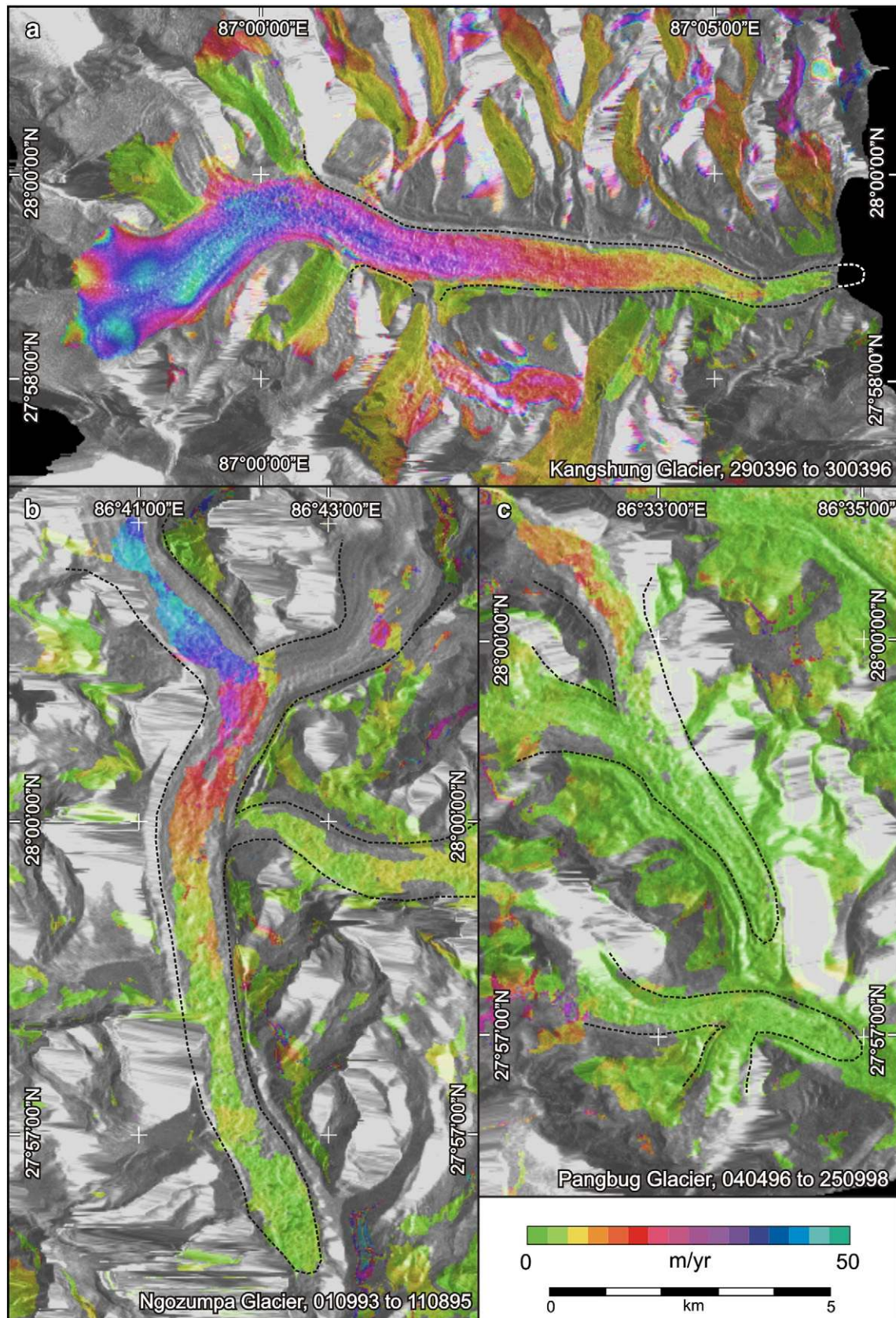
Fig. 6. Surface velocities on Everest region glaciers. Top: Kangshung (Type 1), bottom left: Ngozumpa (Type 2), bottom right: Pangbug Glacier (Type 3). (Modified from Quincey et al., 2009).

glaciers show displacement across the whole surface; Type 2 glaciers show displacement in their upper areas but extensive stagnant or slowly moving ice in their lower ablation zones; and Type 3 glaciers show no clear evidence for displacement anywhere on their surface. The only Type 1 glacier in the sample (n = 20) is Kangshung Glacier, which flows east from the >3 km high Kangshung face of Mount Everest. Velocities increase almost linearly up-glacier, to a maximum measured value of ~35 m yr^{-1}, 8 km from the terminus. (Displacements on higher, steeper parts of the glacier could not be determined.) Twelve of the studied glaciers were of Type 2, with both active and stagnant zones. These glaciers include Ngozumpa Glacier, the lowermost 6.5 km of which is stagnant or almost so. Maximum recorded velocities were ~45 m yr^{-1} in the western tributary, around 5 km upglacier of the transition between active and stagnant ice. Similarly, the lowermost 3–4 km of Khumbu Glacier is stagnant or almost so, above which velocities rise upglacier to >60 m yr^{-1} in the lower part of Khumbu Icefall (Bolch et al., 2008a). The remaining seven glaciers had no detectable motion. These glaciers generally have small accumulation basins and are predominantly fed by avalanching from steep rock headwalls.

Glacier velocity structure shows a clear relationship with catchment elevation. Fig. 7 shows glacier type plotted on a graph of maximum glacier elevation vs. elevation range (Quincey et al., 2009). Entirely inactive (Type 3) glaciers occur exclusively in relatively low catchments, with maximum elevations below ~7250 m, and have the smallest elevation ranges. The Kangshung Glacier (Type 1) has the highest maximum elevation and the greatest elevation range, whereas Type 2 glaciers occupy intermediate positions. The exceptional activity of Kangshung Glacier may also reflect its location on the lee side of Mount Everest. The upper parts of the peak are frequently exposed to high westerly winds, giving rise to the familiar snow plume extending eastward from the summit of the mountain. Unlike the NW and SW faces (above Rongbuk and Khumbu Glaciers, respectively), the Kangshung face consists of a mass of hanging glaciers that feed ice onto the main glacier below. Additional lee-side accumulation, therefore, may have so far buffered Kangshung Glacier from the effects of regional warming.

The distribution of Type 3 and Type 2 glaciers shown in Fig. 7 raises the possibility that stagnant zones will extend farther up many glaciers if the current warming trend continues. Seko et al. (1998) and Nuimura et al. (2011) have presented evidence for a progressive decrease in velocities in the upper ablation zone of Khumbu Glacier since the 1950s. In the zone of prominent ice pinnacles near Everest Base Camp below Khumbu Icefall, for example, velocities decreased from ~56 m yr^{-1} (1956–1978) to ~40 m yr^{-1} (1978–1984) and then to ~20 m yr^{-1} (1995–2004). The area of stagnant ice also appears to have increased slightly between the 1970s and the 1990s (Luckman et al., 2007).

The most likely cause of glacier stagnation and decreasing velocity is the observed reduction of ice thickness and surface gradient over the last few decades (Fig. 5). In addition, many glaciers now have very low gradients in their lower ablation zones (Reynolds, 2000; Bolch et al., 2008a; Quincey et al., 2009). Reduced ice thickness and surface gradient both reduce the driving stress τ_D, given by:

$$\tau_D = \rho_i gH\tan\phi \qquad (2)$$

where ρ_i is ice density, g is gravitational acceleration, H is ice thickness and ϕ is surface slope. Changes to the velocity structure of Everest region glaciers, therefore, appears to be linked to geometric changes, which in turn reflect spatial patterns of melting and accumulation.

6. Mass balance

No systematic direct measurements have been made of glacier ablation or accumulation rates on debris-covered glaciers in the
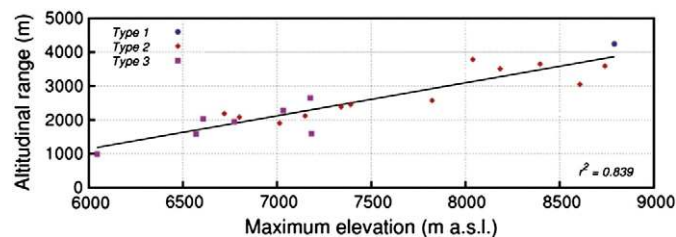
Fig. 7. Plot of glacier elevation range vs. maximum glacier elevation, with three-fold classification of velocity structure. Type 1: active throughout; Type 2: stagnant tongue, active upper part; Type 3: stagnant throughout. (From Quincey et al., 2009).

Everest region. Mass balance data were collected on Glacier AX010, a small clean-ice glacier in the Shorong Himal, in 1989, 1991, and 1995–1999 (Fujita et al., 2001). While this data series is very valuable, the glacier lacks a surface debris cover and spans a small elevation range (~5000 to ~5300 m), and so is not representative of the high elevation, debris-covered glaciers that make up most of the glacier volume in the range (Higuchi et al., 1980).

Snow accumulation rates on the north side of Mount Everest have been reconstructed from an ice core on East Rongbuk Glacier (28.03° N, 86.96° E, 6518 m a.s.l.; Kaspari et al., 2008). The data indicate a current accumulation rate of ~0.45 m yr^{-1} (water equivalent), close to the 500 year mean. Below-average accumulation occurred during the 19th and early 20th centuries, followed by above-average rates during most of the late 20th century. Long-term changes in snow accumulation rates have been linked to variations in northward incursions of the South Asian monsoon (Kaspari et al., 2007).

Only isolated measurements have been made of melt rates on debris-covered ablation zones in the Everest region (e.g. Inoue and Yoshida, 1980; Benn et al., 2001). These measurements were made as part of investigations into local controls on melt rate, and are of very limited duration. Sufficient observations exist, however, to paint a broad picture of the processes controlling glacier mass losses and gains, and to allow theoretical balance gradients to be constructed. On debris-covered glaciers in the Everest region, ice ablation
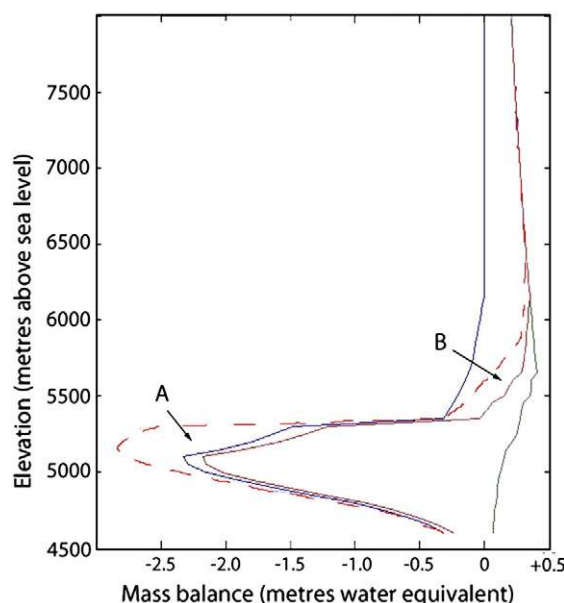
Fig. 8. Modelled annual mass balance gradients for Ngozumpa Glacier. Green: accumulation; blue: ablation; red: net balance. The dashed red line shows the net balance for an increase of 1 °C over the whole elevation range. (For interpretation of the references to colour in this figure legend, the reader is referred to the web version of this article.)

Fig. 9. Supraglacial pond, low-albedo ice faces (dark), and debris-covered ice, Ngozumpa Glacier.

occurs by four main processes: (1) melting of clean ice close to glacier ELAs; (2) melting beneath surface debris; (3) melting of ice cliffs and calving around the margins of supraglacial ponds in the debris-covered area; and (4) calving into deep proglacial lakes (Sakai et al., 1998; Benn et al., 2001; Fujita et al., 2009; Sakai et al., 2009). In this section, we consider processes (1) and (2), together with snow accumulation. Ablation around supraglacial ponds and deep-water calving are discussed in Sections 7 and 9.

In the absence of measured mass balance gradients, we adopt a modelling approach. Although quantitative results of this exercise are subject to high uncertainty, it provides a preliminary framework for understanding glacier response to climate change, and a context for future measurement programmes. Ablation of ice beneath supraglacial debris can be modelled by assuming that energy flux through the debris layer is a purely conductive process driven by energy exchanges at the upper and lower surfaces. Evolution of the heat flux through time is a function of debris temperature and debris-layer properties:

$$\frac{\partial T}{\partial t} = \frac{1}{\rho_d c} \frac{\partial}{\partial z}\left(k\frac{\partial T}{\partial z}\right) \tag{3}$$

where T is temperature (K), ρ_d, c and k are debris layer density (kg m^{-3}), specific heat capacity (J kg^{-1} K^{-1}) and thermal conductivity (W m^{-2} K^{-1}), respectively. When coupled with a surface energy balance model, Eq. (3) can be used to compute melt rates at high temporal resolution (e.g. Reid and Brock, 2010). Implementation of this method requires high-resolution meteorological data and well-known debris layer properties. Where such data are unavailable, a useful approximation can be obtained using 24-hour means of meteorological parameters and a simplified form of the heat flux equation. Surface energy balance can be expressed as:

$$Q_s(1-\alpha) + Q_1 - \varepsilon\sigma T_s^4 + \rho_0\left(\frac{P}{P_0}\right)cAu(T_z - T_s) + \left(\frac{0.622\rho_0}{P_0}\right)LAu(e_z - e_s) \tag{4}$$

$$-k\frac{(T_a - T_i)}{d} = 0$$

(Nicholson and Benn, 2006). The terms on the left-hand side are: net shortwave radiation, incoming longwave radiation, outgoing longwave radiation, sensible heat flux, latent heat flux, and conduction through the debris layer. Individual variables are defined in Table 1. Debris surface temperature appears in the outgoing longwave, sensible heat and conductive terms, and affects the latent heat term through its influence on surface vapour pressure. Eq. (4) can be solved numerically for T_s, and the resulting conductive heat flux used to determine sub-debris melt rate.

This model successfully replicates key features of known relationships between debris thickness and melt rate, and predicts an increase in melt rate (relative to the clean-ice value) where debris cover is thin, and an exponentially decreasing melt rate under thicker debris (Nicholson and Benn, 2006). The first effect occurs because rock debris generally has a lower albedo than either ice or snow (especially when wet), and thus increases net shortwave receipts. The second effect occurs because the debris layer provides an insulating barrier between the ice and the surface. The first effect dominates when the debris is thin, the second when it is thick. Thus, a thin layer of debris accelerates melt rate relative to that of snow and ice, whereas melting is impeded below thicker debris. Modification of the ablation gradient by supraglacial debris will therefore depend upon (1) debris thickness variation with elevation, and (2) vertical meteorological gradients.

As a first approximation, we assume that accumulation is equal to solid precipitation. The vertical gradient of precipitation rate in the Everest region is largely unknown because of a lack of data. Analysis of rain gauges, ERA-40 reanalysis and satellite observations across the Himalaya suggest that there is an approximately exponential decrease of annual precipitation rate with height, limited by available moisture (Kennett and Toumi, 2005). Therefore, the vertical gradient may be approximated by:

$$p(z) \sim p_o \exp(-(z - z_0)/H) \tag{5}$$

where p_o is the precipitation observed at some reference height, z_0. H_v is the saturation water vapour scale height (m):

$$H = \partial z/\ln q_s = T[L_e\Gamma/RT - g/R]^{-1} \tag{6}$$

where T is temperature, L_e is the latent heat of vaporisation (J kg^{-1}), Γ is the temperature lapse rate (K m^{-1}), R is the universal gas constant (J mol^{-1} K^{-1}), g is the acceleration due to gravity (m s^{-2}), and q_s is the saturation water vapour mixing ratio. For the Everest region, a suitable value for H_v is 3.5 km and observed p_o at $z_0 = 5$ km is 0.5 m yr^{-1} (data from Pyramid Station; Bertolani et al., 2000). Solid precipitation is calculated for each altitude from vertical precipitation

Table 1
Definition of symbols used in Eq. (4).

Symbol	Variable
Q_s	Incoming shortwave radiation (W m^{-2})
Q_l	Incoming longwave radiation (W m^{-2})
α	Albedo
ε	Emissivity
σ	Stefan–Boltzmann constant (J s^{-1} m^{-2} K^{-4})
T_s	Ground surface temperature (K)
T_a	Air temperature (K)
T_i	Ice temperature (K)
T_z	Air temperature at elevation z (K)
ρ_0	Reference air density (kg m^{-3})
P	Air pressure (Pa)
P_0	Reference air pressure (Pa)
A	Bulk transfer coefficient
u	Windspeed (m s^{-1})
L	Latent heat of fusion (J kg^{-1})
e_z	Vapour pressure at elevation z (Pa)
e_s	Vapour pressure at surface (Pa)
d	Debris thickness (m)
k	Thermal conductivity (W m^{-2} K^{-1})

gradients and thermal gradients. We adopt the following relationships between the probability of solid precipitation p_s and air temperature T_a (in °C; Ageta and Higuchi, 1984; Kadota et al., 1997):

$$
\begin{aligned}
p_s &= p & (T_a < -0.8°) \\
p_s &= p(0.8 - 0.23 T_a) & (-0.8° \leq T_a \leq 3.4°) \\
p_s &= 0 & (T_a > 3.4°)
\end{aligned}
\tag{7}
$$

Because of the many assumptions made in the formulation and calibration of this model, the results can only provide a general, qualitative picture of actual balance rates in the Everest region. First, the form of the ablation gradient is sensitively dependent on variations in debris layer thickness, thermal properties, and albedo, which are not well known. Second, the model takes no account of melting of bare ice faces or calving into supraglacial ponds, which can introduce large variations to the local melt rate. Third, the model does not include processes that redistribute snow on the glaciers, including wind and avalanching. Fourth, some processes, such as sublimation, are poorly constrained and may be important at high elevations.

In spite of these limitations, we believe the model gives a reasonable view of the general form of the balance gradients of debris covered glaciers, and provides a useful context for discussion of the key drivers of glacier behaviour in this part of the Himalaya. A theoretical mass balance gradient for Ngozumpa Glacier is shown in Fig. 8. The theoretical accumulation maximum is at ~5700 m, representing the crossover point between precipitation totals (which decrease with elevation) and the proportion of precipitation that falls as snow (which increases with elevation). At lower elevations, a proportion of the deposited snow is removed by melting, so that the elevation of maximum net balance lies several hundred metres above the accumulation maximum. The calculated net balance maximum is at ~6200 m, although this can be expected to vary greatly between glaciers depending on aspect, snow redistribution by avalanches, and other factors.

The downglacier increase in debris thickness offsets the effects of higher air temperatures at lower elevations, so that the calculated ablation gradient is inverted on the lower part of the glacier. Again, the elevation at which the reversal occurs, and the maximum ablation rate, will vary depending on model parameterisation and local conditions, but the inversion is likely to be a consistent characteristic of debris-covered glaciers.

The impact of climate change on glacier mass balance was simulated by running the model with a spatially uniform air temperature increase of 1 °C. This has two major effects on the calculated mass balance curve (dashed red line, Fig. 8). First, ablation rates are substantially increased in the mid-ablation zone (A, Fig. 8). If these losses are not replaced by ice advected from upglacier, this will result in increased surface lowering in this area. In contrast, ablation rates undergo little or no change on the lower ablation zone, where debris is thickest. This pattern of ablation is the probable initial cause of the development of concave-up glacier surface profiles that have developed in recent decades (Reynolds, 2000; Bolch et al., 2008b: Fig. 5). Because thinning and reduction in surface gradient reduce the driving stress and decrease velocities (Eq. (2)), patterns of ablation and velocity reduction can be seen as complementary parts of a self-reinforcing cycle of downwasting and stagnation. This cycle will be further reinforced by the formation of supraglacial ponds on low-gradient glacier surfaces, as discussed in the following section.

The second effect of increasing air temperature is a decrease in solid precipitation in the lower part of the accumulation zone (B, Fig. 8). This results from an increase in the elevation of the rain–snow transition, particularly during the warm summer monsoon months. An important implication is that glaciers that have a large proportion of their accumulation areas at relatively low elevations (~5500 to 6500 m) will be especially vulnerable to warming, due to a greater proportion of precipitation falling as rain. Indeed, this appears to be the most likely cause of the observed pattern of glacier activity shown in Fig. 6, in which glaciers in relatively low catchments are most likely to be completely stagnant. Glaciers with greater proportions of their accumulation zones at high elevations can be expected to be less susceptible to stagnation, because ice flux from high-elevation accumulation zones is more likely to maintain active flow in their upper parts (cf. Nuimura et al., 2011).

7. Ablation of bare ice faces and around perched lakes

In debris-covered areas, glacier ice can be exposed around the margins of supraglacial ponds and other hollows on the glacier surface (Fig. 9). Melting and calving of ice cliffs can lead to high rates of ice-cliff retreat or backwasting, contributing disproportionately to glacier ablation. For example, Sakai et al. (2000a, 2000b) found that ice cliffs account for 18% of the ablation in the debris-covered area of Lirung Glacier (~140 km west of Mount Everest), but cover only 2% of the area. On Khumbu Glacier, ice cliffs occupy a similar proportion of the debris-covered area: 2.6% (Sakai et al., 2002). The effect of ice cliffs on local ablation rate can be clearly seen in patterns of glacier elevation change from DEM differencing (Bolch et al., 2011a; Fig. 4).

Ice cliffs form in three main ways: (1) ice becomes exposed by slumping of debris from slopes, (2) calving into supraglacial lakes; and (3) surface subsidence due to the collapse of englacial voids (Kirkbride, 1993; Benn et al., 2001; Sakai et al., 2002). In combination, these processes can lead to an increase in local relief as downwasting proceeds. For example, Iwata et al. (2000) found that the area of high-relief features (20–40 m relative relief) on Khumbu Glacier expanded both up- and down-glacier between 1978 and 1995.

Under clear-sky conditions in the Himalaya, incoming shortwave radiation on suitably oriented ice cliffs can be very high because of low atmospheric attenuation (Benn et al., 2001; Sakai et al., 2002). During the melt season, exposed ice is typically wet and dirty and albedo can be very low (~0.06; Benn et al., 2001), and much of the incoming radiation is available for melting. Longwave radiation emitted from adjacent warm debris surfaces can also be very high. Melt rates are strongly dependent on ice-cliff aspect. Sakai et al. (2002) found that ablation rates were greatest on cliffs oriented east through south, which commonly experience direct insolation in the morning before fog or cloud develops in the afternoon. As a result of high energy receipts, melting ice faces can retreat several metres in a single season (Benn et al., 2001). However, ice faces tend to become less steep through time and become progressively buried by debris derived from upslope. Sakai et al. (2002) showed that ice faces with southerly aspects receive greater incoming shortwave radiation at the top of the slope than the bottom, because of topographic shading effects. As a result, ablation is highest at the top, progressively reducing the slope angle. Slopes <30° rapidly become buried by debris
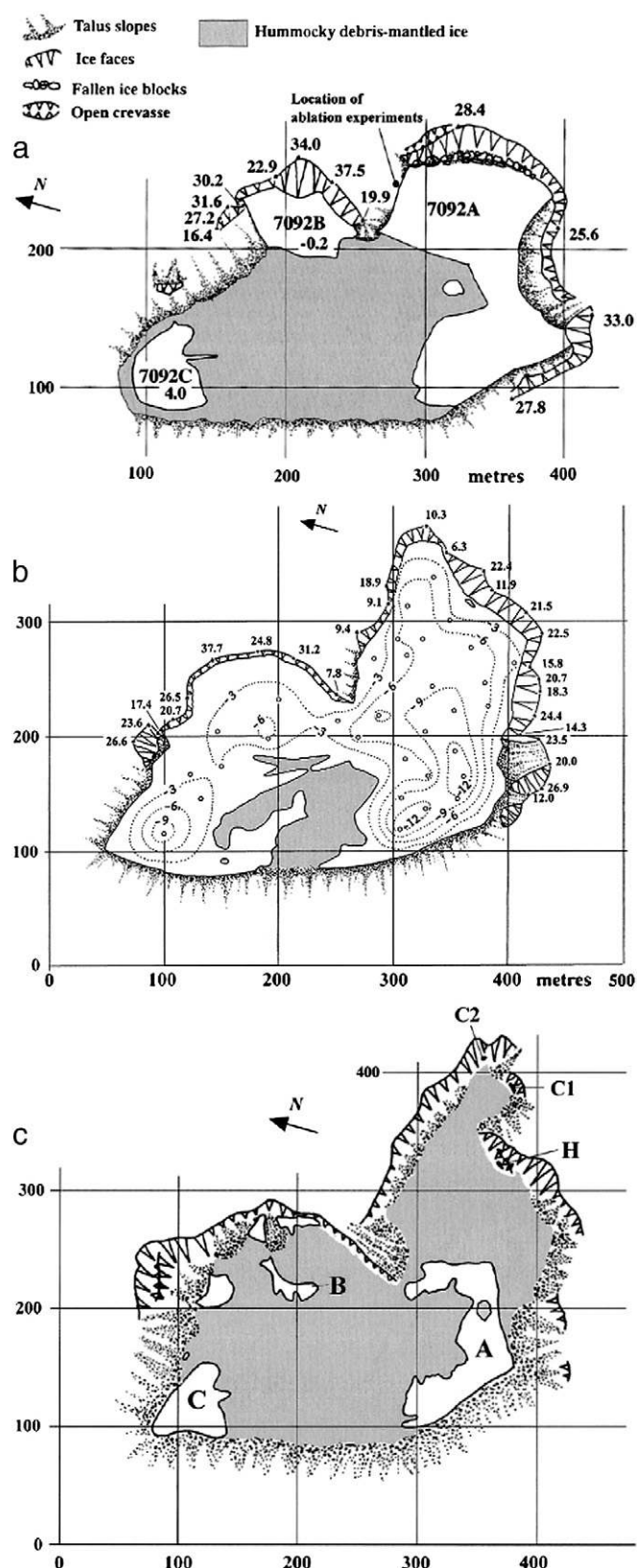
Fig. 10. Evolution of a perched lake, Ngozumpa Glacier, showing lake expansion (1998–1999) and drainage (2000). (From Benn et al., 2001).

falling from the top of the slope, with a consequent large reduction in ablation rates. North-facing ice cliffs tend to be steeper and longer lived, because shortwave radiation contributes less to their energy balance. The process of ice-cliff degradation is important, because it places limits on ablation by cliff backwasting. For melting ice cliffs to persist, topographic relief must be constantly renewed by differential ablation, conduit roof collapse, or calving.

Calving can result in rapid ice loss around the margins of supraglacial ponds, and will continue as long as sufficient water remains in the basin. In a study of two perched lake basins on Ngozumpa Glacier, Benn et al. (2001) found average calving rates of 31 and 51.6 m yr^{-1}, with a maximum retreat rate of almost 100 m yr^{-1}. Total ice ablation in the larger of the two basins was ~300,000 m^3 in a single melt season (Fig. 10). Water from melted icebergs was stored in the lake, and the consequent rise in water level helped to maintain high calving losses. These losses were not sustained, however, because the lake drained via an englacial conduit the following year. Calving losses ceased and ice cliffs became progressively degraded and buried by debris, greatly reducing ablation rates in the basin (Hands, 2004).

Several studies have found that melting at or below the waterline exerts a major control on calving around supraglacial ponds on Everest region glaciers (Benn et al., 2000, 2001; Hands, 2004; Wiseman, 2004; Sakai et al., 2009). Melting undercuts the overlying ice and promotes high stress gradients, encouraging fracture propagation and failure (cf. Iken, 1977; Röhl, 2006a; Benn et al., 2007). During summer and early autumn, observed pond surface temperatures lie in the range 0.7° to 6.6 °C, with a mean of ~3 °C (Wessels et al., 2002; Sakai et al., 2009). When combined with wind-driven lake circulation, subaqueous melt rates can attain several tens of metres per year, an order of magnitude greater than subaerial melt (Sakai et al., 2009). Modelling by Sakai et al. (2009) suggested that calving rates should increase with lake size, through the effect of fetch on windspeed and water circulation. Little data are available to test this prediction, although Hands (2004) found no relationship between ice-cliff orientation and calving rate within a single perched lake basin on Ngozumpa Glacier. She found that many factors influence calving rates, including water depth, height of ice cliff and crevasse distribution, reducing the likelihood that simple calving-rate functions will be found. Waterline melting appears inadequate to explain the calving rates of up to ~50 m yr^{-1} observed at Ngozumpa Glacier. Many of the calving events observed on that glacier involved toppling of large slabs of ice along pre-existing crevasses. This process is important where ice cliffs exceed 15 m in height, perhaps because some threshold stress gradient is required to reactivate suitably oriented crevasses.

Perched lakes can only persist when underlain by intact, unfractured glacier ice, which has very low permeability (Jordan and Stark, 2001). Lake drainage will occur when water is able to exploit permeable structures in the ice, such as active or relict englacial conduits, or debris-filled crevasse traces (Benn et al., 2001; Gulley and Benn, 2007; Gulley et al., 2009b; Fig. 11). The spacing of such structures in debris-covered glaciers in the Everest region is such that perched lakes rarely persist for more than a few years before draining. Some lakes undergo several cycles of drainage and refilling, causing regions of high ablation to switch on and off repeatedly. Detailed reconstructions of several perched lake drainage events have been made possible by speleological investigations of englacial conduits, described in the following section.

8. Glacial drainage systems

Glacial drainage systems exert a strong control on the life cycle of perched lakes, by facilitating both lake drainage and the initiation of new lake basins. In recent years, several englacial conduits in Everest-region glaciers have been explored and mapped using speleological techniques, with surveys conducted during the winter season when conduits are largely empty of water (Gulley and Benn, 2007; Benn et al., 2009; Gulley et al., 2009a, 2009b). In this section, we review knowledge of drainage systems in debris-covered glaciers in the Everest region, and explore how coupling between surface and subsurface processes influences glacier evolution.
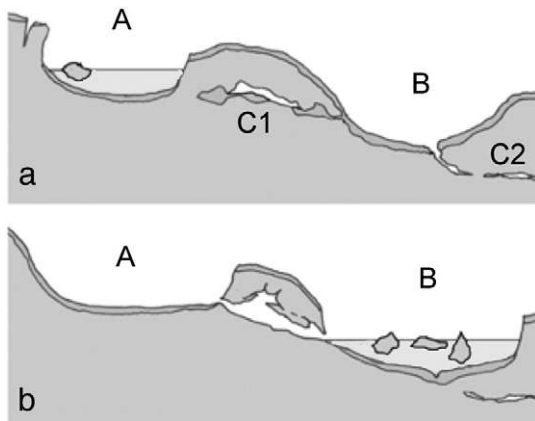
Fig. 11. Schematic diagram of perched lake drainage. a) Lake A is underlain by intact glacier ice; Basin B formerly contained a lake that drained through conduit C2. b) Ice-cliff retreat in Basin A brought the lake into contact with partially debris-filled conduit remnant C1, allowing water to flow into Basin B where hydraulic potential is lower. Conduit C2 has become blocked, retaining water in the basin. Rapid ice-cliff retreat is switched off in Basin A and switched on in Basin B.

Fig. 12. Supraglacial meltwater channels on Rongbuk Glacier. North is to the bottom of the image, and the scale bar represents 1 km. (Google Earth).

In common with alpine glaciers elsewhere, Himalayan glaciers can have supraglacial, englacial and subglacial drainage system components. Perennial supraglacial channels exist on many debris-covered glaciers in the Everest region. Channels will persist from year to year where the annual amount of channel incision exceeds the amount of surface lowering of the adjacent ice, so their distribution reflects the factors controlling the relative rates of these processes (Gulley et al., 2009a). The incision rate $\dot{d}$ (m s^{-1}) for ice-floored channels is determined by viscous heat dissipation associated with turbulent flow, and increases with surface slope S and discharge Q (m^3 s^{-1}):

$$\dot{d} = \frac{1}{2}\left(\frac{\pi}{2\bar{n}}\right)^{3/8}\left(\frac{\rho_w}{\rho_i}\right)\left(\frac{g}{L}\right)S^{19/16}Q^{5/8} \qquad (8)$$

where $\bar{n}$ is Manning's roughness (s m$^{-1/3}$), ρ_w and ρ_i are the densities of water and ice, respectively (kg m^{-2}), and L is the latent heat of melting (Fountain and Walder, 1998). Surface melt rates tend to be small on thickly debris-covered Himalayan glacier tongues (Section 6), and because supraglacial stream discharge is a function of melt rate and catchment area, it follows that significant channel incision requires large catchment areas. Therefore, deeply incised surface channels tend to occur where potential catchments are not fragmented by crevasses or other wells on the glacier surface. These conditions are met on the upper ablation zones of several debris-covered glaciers in the Everest region, where extensive supraglacial channel networks can be found. An example from Rongbuk Glacier is shown in Fig. 12. On many glaciers, the lower ablation zone is broken up into numerous closed basins, and catchments are too small for deeply incised streams to develop. Consequently, integrated networks of supraglacial streams are not found and surface meltwater tends to flow in small, ephemeral rills.

Speleological surveys have yielded evidence for three fundamental processes of englacial conduit formation on Himalayan glaciers: (1) 'cut-and-closure', or incision of supraglacial streams followed by roof closure; (2) exploitation of lines of secondary permeability; and (3) propagation of water-filled fractures (hydrofracturing) (Gulley and Benn, 2007; Benn et al., 2009; Gulley et al., 2009a).

Cut-and-closure conduits evolve from supraglacial stream channels following roof closure by a combination of ice creep and blockage by snow, ice and debris. The cut-and-closure process initially produces simple, meandering canyon-like passages with low overall gradients, trending approximately parallel to the ice surface. Through time, conduit morphology can undergo major changes in response to competing processes of tunnel enlargement and closure (Fig. 13). Because they evolve from supraglacial channels, cu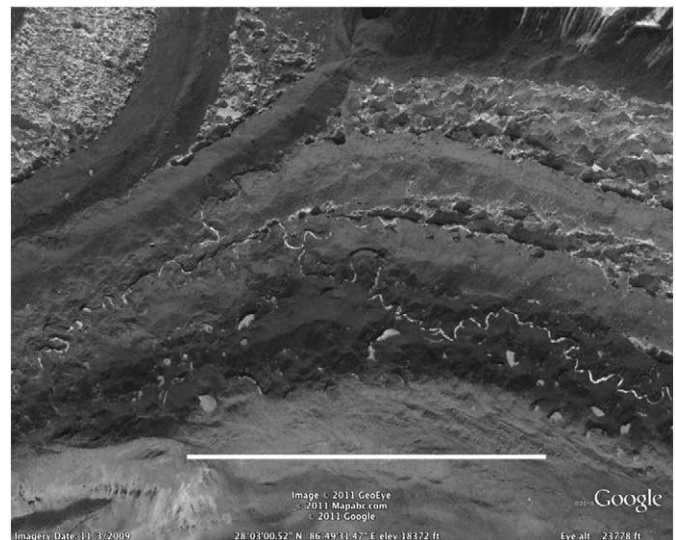t-and-closure conduits initially form where catchments are relatively large and uninterrupted by crevasses or closed depressions on the glacier surface. Such conduits can, however, persist at depth after surface catchments have been broken up by differential ablation during glacier downwasting. Some cut-and-closure conduits extend the full length of glaciers, and transfer water from the upper ablation zones to the terminus, bypassing large parts of the lower ablation zones. Examples of active cut-and-closure conduits near the terminus of Ngozumpa Glacier have been described by Thompson et al. (2012).

Uneven surface ablation on debris-covered glaciers can lead to fragmentation of cut-and-closure conduits, cutting off downstream reaches from major sources of recharge. When water inputs are lost, passage closure processes dominate over processes of passage enlargement, and abandoned conduits gradually close down. Incomplete shutdown of abandoned reaches of cut-and-closure conduits can leave networks of open voids and porous debris fills in otherwise intact glacier ice. Gulley et al. (2009a) described two cut-and closure conduits that had been abandoned following the loss of former water sources.

Conduit formation along lines of secondary permeability appears to be a very widespread process on debris-covered glaciers in the Everest region, particularly on stagnant glacier tongues. Gulley and Benn (2007) argued that sand and gravel infills of former surface crevasses create networks of permeable structures through otherwise impermeable ice, which can be exploited and enlarged by meltwater. Although crevasse traces appear to be locally important, recent unpublished observations by the authors show that abandoned cut-and-closure conduits are probably a much more important cause of secondary permeability, due to their greater continuity.

Remnants of cut-and-closure conduits are particularly important as pathways for the drainage of perched lakes. When the expansion of a lake brings it into contact with a relict conduit, water can be driven out along the structure if it connects with a region of lower hydraulic potential (Gulley and Benn, 2007). On an irregular glacier surface, this can occur where relict conduits bridge between a water-filled basin and a lower hollow (Fig. 11). The drainage of warm lake waters along permeable structures causes internal ablation, opening up voids within the glacier (Fig. 14). Additional void enlargement can occur when ice blocks fall from the conduit roof and are later removed by water flow. Through time, voids tens of metres across and several metres high can develop, increasing the likelihood of roof collapse and surface subsidence. This process exposes bare ice at the surface, creating new zones of enhanced ablation. If the parent conduit becomes blocked,

Fig. 13. Englacial conduit morphology. a) Vertical-walled canyon with roof suture, Khumbu Glacier. b) Tubular passage with incised floor, formed by re-activation of a relict conduit, Ngozumpa Glacier.

regions of subsidence can become flooded, and evolve into new supraglacial ponds, further increasing local ablation rates.

The third process known to form englacial passages in Himalayan glaciers is hydrologically assisted propagation of water-filled crevasses, or hydrofracturing (Benn et al., 2009). Surface crevasses usually do not penetrate to great depth, because any tensile stresses tending to pull the crevasse open are increasingly opposed at depth by ice overburden pressure (Van der Veen, 1998). The presence of water in a crevasse offsets the overburden pressure, allowing the crevasse to propagate to greater depths. If sufficient water is available to recharge an advancing fracture, this process can rapidly route surface water to glacier beds, even through great thicknesses of cold ice (Alley et al., 2005; Van der Veen, 2007).

Englacial conduit formation by hydrofracturing appears to be spatially restricted on the debris-covered areas of Himalayan glaciers, occurring where supraglacial ponds coincide with areas of compressive stress (Benn et al., 2009). In 2005 and 2006, two examples occurred ~5 km upglacier from the terminus of Khumbu Glacier, where active ice decelerates against the stagnant lower tongue. Compressive ice flow in this region results in transverse extension of the ice and the development of longitudinal fractures, and the conduits formed where such fractures were accessed by water from supraglacial ponds. The larger of the conduits was almost 35 m high and 120 m long.

Very little is known about the subglacial components of Himalayan drainage systems, and with one or two minor exceptions, direct

Fig. 14. Surface subsidence on Ngozumpa Glacier, 1999. This area later evolved into a chain of supraglacial ponds. Figure (circled) for scale.

speleological observations are lacking. Seasonal velocity fluctuations on some of the large glaciers in the Khumbu region (Kodama and Mae, 1976; Quincey, 2006) imply that, in the upper parts of some glacier ablation zones, surface water is routed efficiently to the bed. By analogy with other areas, the most likely mechanism is hydrologically assisted crevasse propagation in icefalls and other regions of high strain (cf. Benn et al., 2009). The high altitude and unstable nature of Himalayan icefalls, however, mean that this speculation is likely to remain untested by speleological methods.

9. Base-level lakes

If a supraglacial lake develops at the same elevation as the lowest point of a terminal moraine dam, it will not drain until the dam is lowered, either by gradual incision of the outlet or catastrophic failure. Unlike perched lakes, therefore, base-level lakes can continue to grow for several decades and attain large volumes ($>10^8$ m^3). Such large lakes can pose significant GLOF hazards if vulnerable moraine dams coincide with potential trigger mechanisms such as ice avalanches or rock-slope failures into the lake (Reynolds, 1998; Yamada, 1998).

Base-level lake formation depends on the presence of a continuous moraine loop around the glacier terminus. The presence of a continuous moraine depends on long-term depositional conditions at the glacier terminus, particularly the balance between debris accumulation and glacifluvial sediment evacuation. Moraine will accumulate where meltwater fluxes are insufficient to transport the available debris away from the glacier terminus, whereas efficient glacifluvial debris transport will tend to maintain open corridors around major meltstreams. The conditions for moraine formation reflect the degree of coupling between glacial and glacifluvial sediment transport systems. Moraine accumulation is favoured at *decoupled margins*, where there are weak linkages between the glacial and glacifluvial systems, and discouraged at *coupled margins*, where glacial debris is efficiently evacuated by glacifluvial processes (Benn et al., 2003). Decoupled margins occur on glaciers with large loads of rock debris and relatively low meltwater runoff, which typically occur in regions with high relief and low summer temperature. These conditions are met in the Everest region, where most debris-covered glaciers have decoupled margins. There are some exceptions, however, mainly depending on local topography. Lhotse Glacier, for example, has a coupled margin and meltwater can be progressively lost from the system during periods of negative mass balance, with little or no potential for significant storage in a base-level lake.

Where a continuous moraine loop is present, a base-level lake will develop once part of the glacier surface down-wastes to the level of the spillway through the moraine. Base-level lakes typically begin as groups of small ponds, which gradually coalesce into a single lake. For example, ponds began to form on the lower tongue of Trakarding Glacier in the 1950s, and had coalesced into a single base-level lake (Tsho Rolpa) by the 1960s (Reynolds, 1998). The lake continued to expand up- and downglacier, and by 2006 had an area of 1.5 km^2 (Sakai et al., 2009). Similarly, the lake Imja Tsho on Imja–Lhotse Shar Glacier began as a series of small ponds in the 1950s, and had developed into a single water body by the 1970s (Fujita et al., 2009; Watanabe et al., 2009). The early stages of the evolution of a base-level lake on Ngozumpa Glacier ('Spillway Lake') have been documented by Benn et al. (2001) and Thompson et al. (2012). Repeat field surveys and satellite image analysis show that patterns of lake expansion are strongly preconditioned by the location of shallow englacial conduits, which provide a dendritic template for the evolving lake planform (Fig. 15). As the overlying ice thins, the roofs of cut-and-closure conduits collapse, creating linear zones of subsidence on the glacier surface. These then evolve into chains of ponds, which expand by melt and calving of exposed ice around their margins. Through time, ponds coalesce and intervening promontories and islands are removed by ablation on all sides.

The growth of moraine-dammed lakes also involves removal of ice from below the lake floor as well as around its margins. Very little is known about processes and rates of lake-floor deepening, although two processes are thought to be important. First, melting occurs by heat conduction through lake-floor sediments (Chikita et al., 1999, 2001; Hands, 2004). At Tsho Rolpa, Chikita et al. (1999) found that a combination of wind-driven surface currents and density-driven underflows creates vigorous circulation in the lake, delivering energy to the subaqueous ice front and lake floor, melting the ice. The second process of lake-floor deepening is subaqueous calving, which could remove large blocks of fractured ice in a series of discrete events. Based on observations of lakes at the debris-covered Tasman Glacier, New Zealand, Röhl (2006b) argued that the onset of subaqueous calving is a crucial process for the transition to faster disintegration and ice loss, which in turn accelerates subaqueous melt. It is possible that similar processes occur on Himalayan glaciers, although additional observations are needed before a quantitative understanding of lake-floor deepening can be achieved.

Base-level lakes can grow both downglacier and upglacier, with different implications for lake evolution and stability (Watanabe et al., 2009). Downglacier lake growth tends to occur by degradation of debris-covered, stagnant ice rather than calving, and is generally slow. Downglacier lake growth, however, has the effect of narrowing the lake dam, increasing the risk of failure. Upglacier lake growth occurs by retreat of the glacier front, and can cause rapid increase in lake volume and area, particularly if retreat occurs by deep-water calving (cf. Kirkbride and Warren, 1999). Little is known about the processes of calving into Himalayan moraine-dammed lakes, although it is likely that several processes are involved, including opening of transverse crevasses by longitudinal stretching, and uplift and detachment of buoyant parts of the glacier tongue (cf. Benn et al., 2007).

Rates of growth have now been determined for several lakes in the Himalaya (Fig. 16, Komori et al., 2004; Sakai et al., 2009; Thompson et al., 2012). For many of the lakes, periods of rapid growth are interrupted by periods of slow growth or even reductions in area. In all cases, however, these are temporary pauses in the overall trend of increasing area. For the sampled lakes, long-term growth rates are remarkably similar, and mostly lie in the range 0.02 to 0.03 km^2 yr^{-1}. The area of a lake at any given time is likely to be the result of many factors, such as timing of lake initiation, glacier activity and mass balance. In the Khumbu Himal, there is a broad tendency for the largest lakes to be located at relatively low elevations (4500–5000 m), on glaciers with large elevation ranges (Fig. 17). This pattern may partly be a function of the area available for growth (the glaciers with the greatest elevation ranges are also the largest), but could also reflect the greater climatic sensitivity of relatively low-elevation glacier fronts.

10. Glacier lake outburst floods (GLOFs) from base-level lakes

Lake area and expansion rates are poor indicators of GLOF hazard potentials, and hazard predictions based on these factors alone can promote needless alarm and suspicion among local people (Watanabe et al., 2009). Many factors contribute to the likelihood of dam failure, including dam height, width and composition, and the probability of trigger events (Richardson and Reynolds, 2000; Huggel et al., 2004). Balanced assessment of present and future GLOF hazards in the Everest region, therefore, requires a synoptic viewpoint, including knowledge of glacier mass balance, dynamics, hydrology, and controls on dam geometry and stability.

A major factor determining GLOF hazard potential is the hydraulic gradient across the moraine dam, which influences its susceptibility to seepage. Hydraulic gradient is determined by the geometry of the dam (especially the freeboard and the ratio of dam width to height), so narrow, high dams with low freeboard are most likely to fail. In addition, failure of dams becomes increasingly likely as moraines degrade
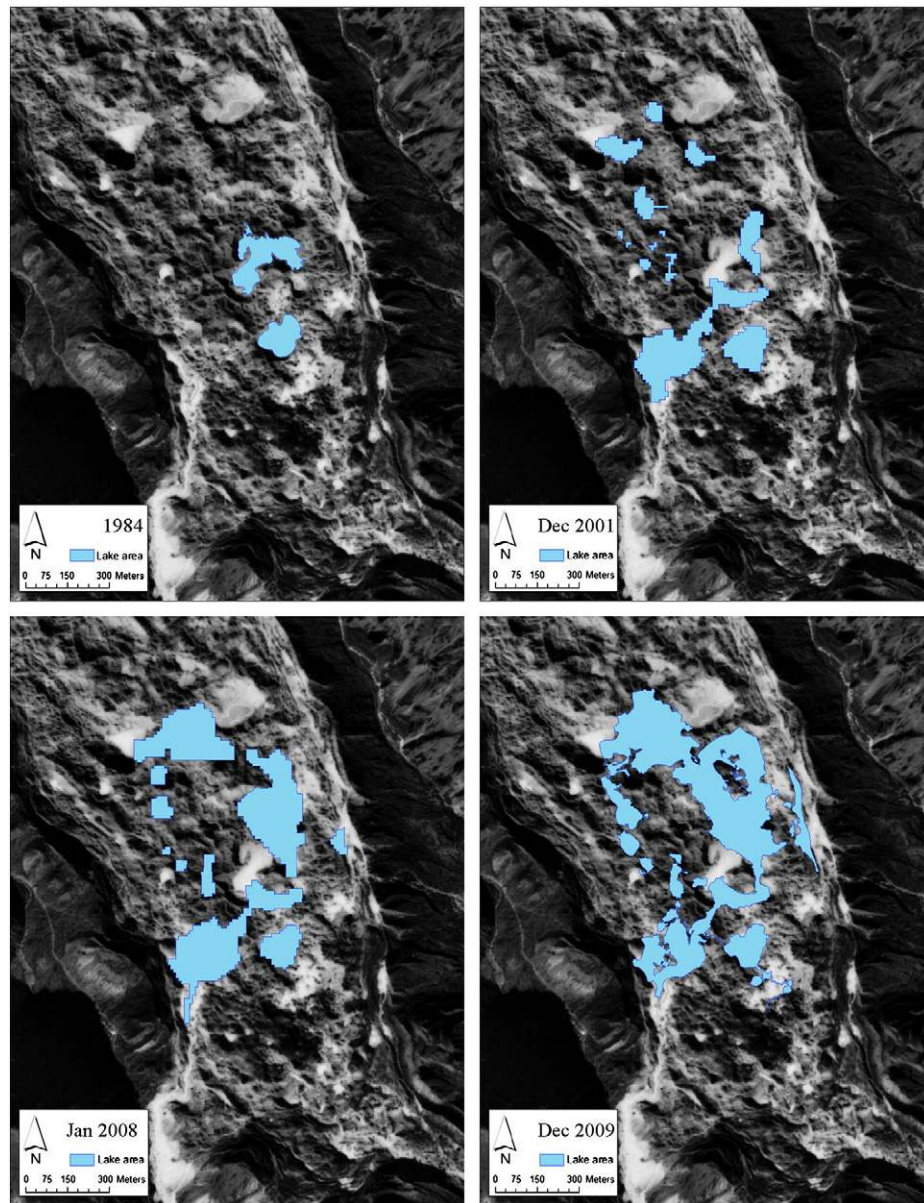
Fig. 15. Growth of Spillway Lake, Ngozumpa Glacier, from 1984 to 2009. (From Thompson et al., 2012).

due, for example, to melt of buried ice (Richardson and Reynolds, 2000). In high mountain environments such as the Himalaya, the most important trigger mechanisms are rock or ice avalanches. These can cause seiche waves that overtop and erode moraine dams, initiating a positive feedback of discharge and erosion. For example, the 1985 outburst of Dig Tsho was triggered by a major ice avalanche from an icefall on Langmoche Glacier, which entered the lake after travelling over an area of stagnant ice and snow (Vuichard and Zimmermann, 1987). Extreme meteorological events, such as prolonged heavy rain or periods of exceptional melt, have also been known to trigger outburst floods. Scoring systems have been developed for GLOF hazard assessments, based on the idea that weightings can be assigned to a range of risk parameters such as lake volume, moraine dam geometry, and the location of source areas for ice and rock avalanches (Reynolds Geo-Sciences, 2003; Huggel et al., 2004; Bolch et al., 2011a). Such schemes bring a much-needed systematic, rational approach to GLOF hazard assessment.

The importance of site-specific factors in GLOF hazard assessment can be illustrated by comparing two well-known examples, Imja Tsho on Imja–Lhotse Shar Glacier and Tsho Rolpa on Trakarding Glacier, both of which have grown rapidly in area since inception in the 1950s. The lake

dams are very different in character, with major implications for relative GLOF hazard potential. Imja Tsho is dammed by a belt of debris-covered ice some 500 m across, through which water drains via an ice-floored channel (Hambrey et al., 2008; Watanabe et al., 2009). Incision of the channel has lowered lake level by 37 m over the last 4 decades, a process that could eventually allow the lake to drain gradually and safely (Watanabe et al., 2009; Fig. 18). The ice dam is gradually becoming narrower, however, and there are indications that the ice-floored channel is evolving into a new arm of the lake. The long-term hazard potential, therefore, depends crucially on the balance between incision and narrowing of the ice dam. If the former dominates, the lake may completely drain safely, whereas if the latter dominates, catastrophic drainage may occur. There appears to be no immediate danger of lake drainage, although continued monitoring is advisable.

In contrast, Tsho Rolpa is dammed by a narrow, steep-fronted, partially ice-cored moraine (Richardson and Reynolds, 2000). Like Imja Tsho, the lake is not threatened by hanging glaciers on the surrounding mountainsides, although calving from the active glacier front poses some risk of seiche waves. At Tsho Rolpa, the lack of freeboard at the terminal moraine meant that even relatively small events
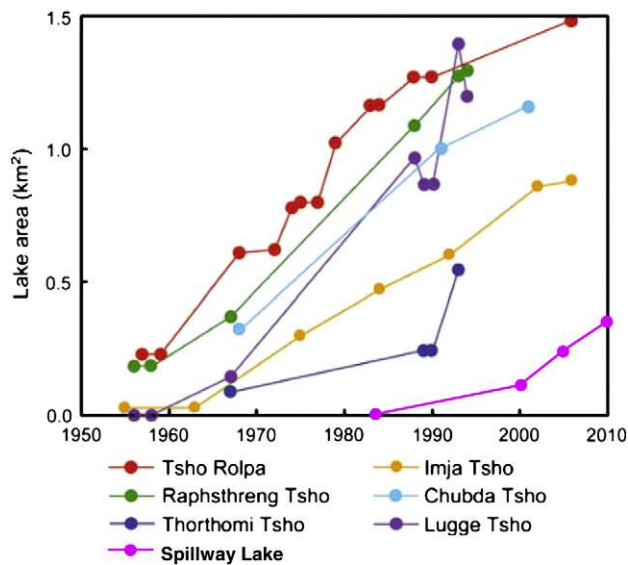
Fig. 16. Growth of Himalayan base-level lakes. (From Thompson et al., 2012, after Komori et al., 2004; Sakai et al., 2009).

could trigger dam incision and failure. In view of these factors, a hazard assessment exercise in the 1990s concluded that Tsho Rolpa posed a considerable danger of a GLOF, and an early warning system was installed (Reynolds, 1998; Rana et al., 2000). In 1998–2000, a coffer dam and artificial spillway were constructed, lowering lake level by 3 m. These measures, which cost $2.7 million, have reduced but not removed the danger of a GLOF, and additional lowering by perhaps 10 to 20 m is considered necessary to reduce the danger to a 'modest level' (Kattelman, 2004). The logistical difficulties and high costs of such measures emphasise the importance of careful risk assessment including the vulnerability of downstream areas.

11. Marginal lakes

In high relief areas, temporary lakes can also form where drainage from side- or trunk valleys is blocked by glacier ice or moraine (Clague and Evans, 2000). Along the western margin of Ngozumpa Glacier, for example, a series of lakes have been dammed in side valleys by the right-lateral moraine of the glacier. These lakes now stand tens of metres higher than the adjacent downwasting glacier surface, so they will drain if the moraine dam is breached.
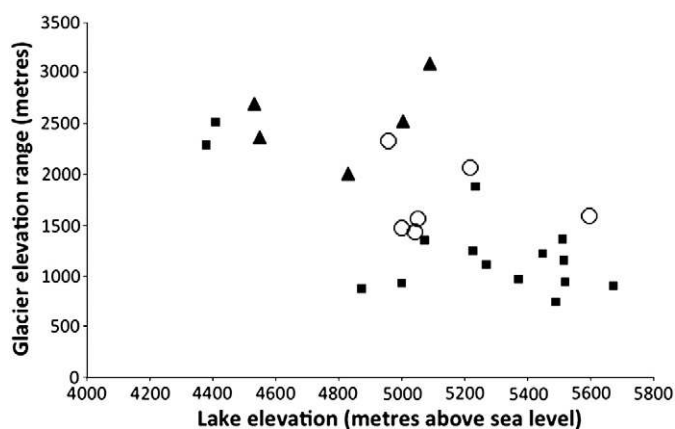

Fig. 17. Base-level lake elevation vs. glacier altitudinal range. Lake area is indicated by symbol: squares = <0.5 km²; open circles = 0.5 to 1.0 km²; triangles = >1.0 km².

The lateral moraine barrier at Ngozumpa Glacier is currently 200 to 500 m wide, with a strongly asymmetric cross-profile. The ice-distal slopes were formed by debris flow and glacifluvial processes when the glacier margin stood above the moraine crest, and have generally low gradients (<30°) and a mature vegetation cover. In contrast, the ice-proximal slopes are unvegetated and actively retreating, and consist of a near-vertical upper slope and a less steep lower slope of accumulated debris. Erosion of the moraine dam, therefore, is predominantly controlled by retreat of its ice-proximal side. Rates of slope retreat were measured over a two-year period by Hands (2004). Retreat rates ranged from 0 to ~2 m yr^{-1}, with an overall mean of 0.48 m yr^{-1}. In some areas, more rapid erosion occurred by landslipping, where slippage of blocks removed slabs of moraine several metres across in a single year. Long-term erosion rates from landslipping depend on the recurrence interval of events, which is unknown. At the measured rates, removal of the moraine barrier would take several hundred years, indicating there is no immediate risk of drainage of these lateral lakes. In the longer term, however, lake drainage appears to be inevitable if glacier retreat continues and the landscape progressively relaxes into a non-glacial state.

12. Evolution of debris-covered glaciers

The development of potentially unstable moraine-dammed lakes is one possible end product of the wastage of debris-covered glaciers. Whether lakes develop or not, and whether they pose significant risks to downstream populations, depends on the particular sequence of geometric, dynamic, and hydrological changes that occur, which in turn depend on site-specific climatic, topographic and glaciological conditions. Knowledge of these conditions, and their linkages to glacier response, can therefore underpin long-term hazard assessments. In this section, we outline a general conceptual model of the evolution of debris-covered glaciers during periods of negative mass balance (Fig. 19). An important aspect of this model is the recognition of threshold behaviour, in which glaciers can undergo major transitions in dynamics, mass loss rates, and processes and patterns of water storage. Three process regimes can be identified, transitions between which represent major thresholds in glacier response to climate forcing.

12.1. Regime 1: Active ice flow, low water storage

In regime 1, all parts of the glacier are dynamically active. Ablation is predominantly by melting beneath surface debris although melting of bare ice faces or around small, ephemeral ponds may make some contribution. Debris typically increases in thickness downglacier, insulating the underlying ice and offsetting the effects of higher air temperatures at lower elevations. As a result, ablation gradients are typically reversed in lower ablation zones, with melt rates declining to very low values near glacier termini (Nakawo et al., 1999; Benn and Lehmkuhl, 2000; Nicholson, 2005). The highest melt rates typically occur in the mid-ablation zones, where debris cover is thin. For a glacier to maintain zero net balance, ice flux into the upper- and mid-ablation zones must be sufficient to compensate for losses by melting. Prior to 20th century warming, the majority of glaciers in the Everest region may have been in regime 1. Few remain in that regime at the present time, a notable example being Kangshung Glacier.

On the larger glaciers, drainage systems might consist of supraglacial, shallow englacial, and subglacial components, whereas on smaller glaciers the subglacial component may be missing. Where the glacier surface is not extensively crevassed, surface meltwater can be transported to the glacier terminus in either surface channels or englacial cut-and-closure conduits. The key characteristic of the drainage systems of active debris-covered glaciers is that meltwater should be routed efficiently out of the glacier system with little multi-annual storage. Water can, however, be dammed in side valleys by ice or moraine (cf. Clague and Evans, 2000).
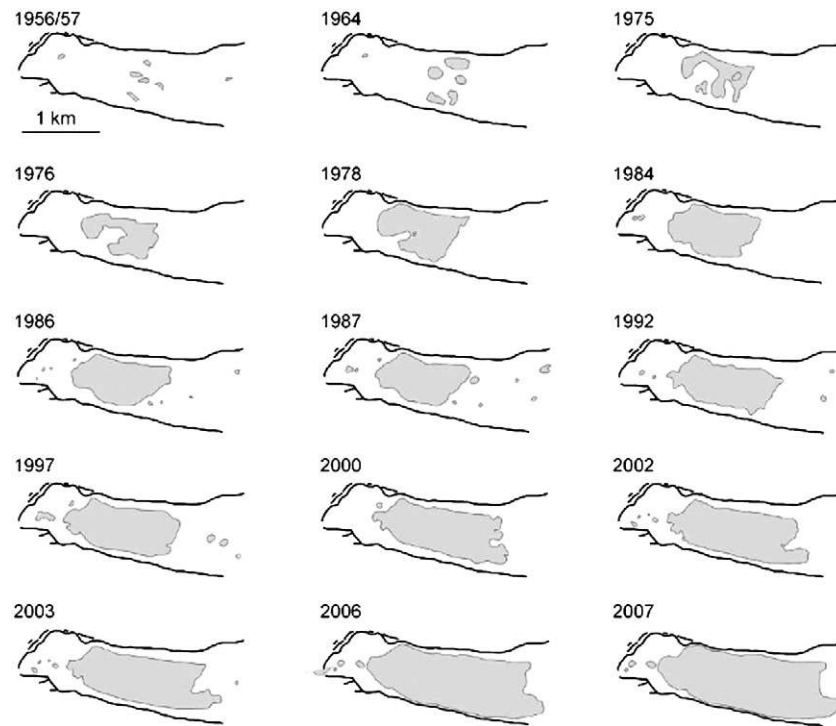
Fig. 18. Development of Imja Tsho, 1956/7 to 2007. (From Watanabe et al., 2009).

12.2. Regime 2: Downwasting ice, distributed water storage

Climatic warming can critically alter the balance between ice influx and ablation rates on debris-covered glacier tongues, in some cases leading to a transition to regime 2 and a qualitative change in glacier behaviour. Higher temperatures (particularly summer temperatures) can result in both an increase in the elevation of the rain–snow boundary, reducing solid precipitation, and higher melt rates. In consequence, mid-ablation zones will experience both increased mass loss and reduced ice flux from upglacier. Relatively high rates of surface lowering in the mid-ablation zone (due to the influence of debris cover on the ablation gradient) cause a reduction of the glacier surface gradient and the creation of a characteristic concave-up long profile (Reynolds, 2000; Bolch et al., 2008b, 2011a). In turn, this results in reduced driving stresses in the lower ablation zone, encouraging glacier slowdown and stagnation (Quincey et al., 2009).
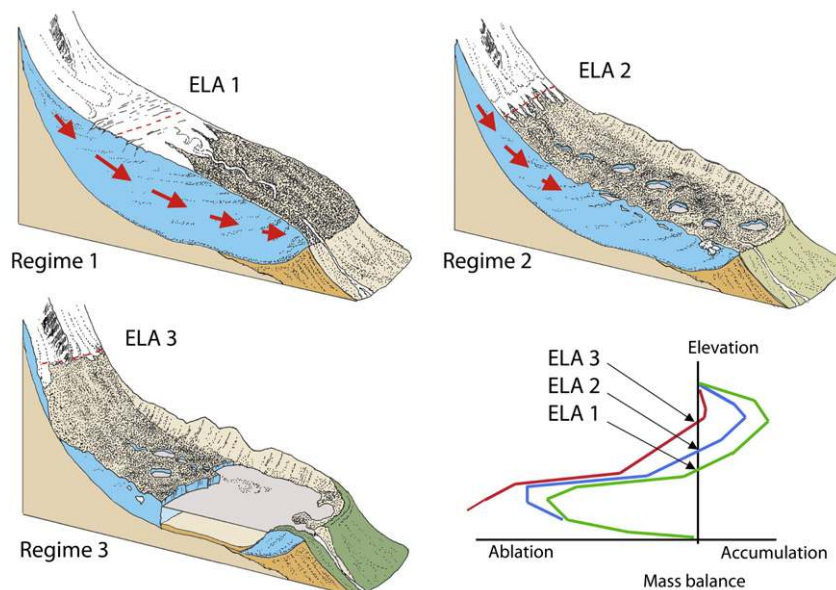

Fig. 19. Schematic representation of Himalayan debris-covered glacier ablation regimes and velocity structures. Note that glaciers with base-level lakes (regime 3) can have both actively flowing and stagnant ice (velocity type 2) as well as entirely stagnant ice (velocity type 3), as shown. The bottom left panel shows idealised mass balance curves and equilibrium line altitudes (ELAs) for ablation regimes 1 (green), 2 (blue) and 3 (red). (For interpretation of the references to colour in this figure legend, the reader is referred to the web version of this article.)

Reduction of glacier gradient also brings about profound changes in glacier hydrology. Several studies have shown that the distribution of supraglacial lakes is strongly related to glacier surface gradient ϕ (e.g. Reynolds, 2000; Bolch et al., 2008b; Quincey et al., 2009; Sakai and Fujita, 2010). For debris-covered glaciers in Bhutan, Reynolds (2000) found that all surface water is able to drain away where $\phi > 10°$, small ephemeral ponds form where $10° > \phi > 6°$, supraglacial ponds are widespread where $6° > \phi > 2°$, and large lakes can form where $2° > \phi > 0°$. Water storage is also encouraged by the breakup of formerly integrated drainage systems by uneven surface ablation. The dismemberment and abandonment of former cut-and-closure conduits essentially switches off efficient evacuation of meltwater, allowing ponds to form in closed hollows on glacier surfaces. Ablation around lake margins by calving and melting is typically one or two orders of magnitude higher than that for adjacent debris-covered ice, so extensive pond formation locally accelerates downwasting rates (Sakai et al., 1998; Benn et al., 2001). Enhanced ablation around perched lakes ceases, however, when lakes drain via relict cut-and-closure conduits and other sources of secondary permeability.

In regime 2, therefore, an initial climate signal is amplified by a positive feedback loop, in which mutually reinforcing patterns of surface lowering, ice stagnation and water storage serve to accelerate ice loss.

12.3. Regime 3: Calving retreat, high water storage

Where a continuous terminal moraine loop prevents free drainage of meltwater, base-level lakes can form once part of the glacier surface is lowered to the lowest point of the dam. Intersection of the downwasting glacier surface with an elevated base level, therefore, is a very important process threshold that is necessary for the formation of base-level lakes. Base-level lakes can expand rapidly by calving and melting above or below the waterline, and patterns of lake growth may be strongly conditioned by lines of weakness provided by shallow englacial conduits. Lake growth can continue unchecked while the moraine dam remains in place, and volumes of stored water can attain $\sim 10^7$ m^3 of water (e.g. Imja Lake: Fujita et al., 2009; and Tsho Rolpa: Sakai et al., 2000b). In their early stages, base-level lakes occupy supraglacial positions, and grow by processes similar to those associated with perched lakes (Benn et al., 2001; Lamsal et al., 2011; Thompson et al., in press). Progressive lake deepening, however, will eventually cause the lake floor to contact the former glacier bed. The transition from supraglacial lake to full-depth lake is another important threshold, after which rapid lake growth can occur by deep-water calving (Kirkbride, 1993; Kirkbride and Warren, 1999).

Transition of glaciers from regime 2 to regime 3 depends on the existence of a 'decoupled margin' (Benn et al., 2003). Because decoupled margins reflect the long-term balance between supraglacial debris supply and meltwater runoff, their distribution will reflect both regional and local climatic and topographic factors. Therefore, we should expect to find clusters of susceptible glaciers in particular regions. The Everest region provides an excellent example of one such cluster.

13. Prediction of GLOF hazard

The existence of large base-level lakes does not, in itself, provide sufficient evidence of potential GLOF hazard. The danger of dam failure depends on the nature of the dam (geometry, composition and freeboard), and the presence or absence of potential trigger mechanisms. Large lakes can exist in the landscape for long periods if they are dammed by a stable barrier such as a broad outwash fan, or drain gradually if the downcutting of the outlet proceeds slowly and steadily.

The formation of new base-level lakes can be predicted by identifying glaciers that are in an advanced stage of regime 2. That is, glaciers with concave-up long profiles, very low surface gradients in the terminal zone, large areas of stagnant ice, and elevated hydrological base levels provided by large terminal moraines (Quincey et al., 2007; Fig. 19). The correspondence between glacier activity and elevation (Fig. 7), suggests that the geometric evolution of glaciers in regime 2 is modulated by climatic and topographic factors, providing an additional basis for predictions. Glaciers that are already completely stagnant (Type 3 glaciers) are nourished in comparatively low catchments, where rising summer temperatures and increasing elevation of the monsoon rain–snow transition have the largest effect on glacier mass balance. The combined impact of increased ablation and reduced accumulation cause accelerated mass loss and reduced ice discharge on the ablation zones, to the extent that the remaining tongues of Type 3 glaciers are now relict and are wasting away in situ. Type 2 glaciers are nourished at higher elevations, and still have enough snow accumulation at high elevations to sustain some ice flow into their ablation zones. Further analysis of the activity and hypsometric characteristics of Type 2 glaciers may provide an additional means of identifying potential sites of new base-level lakes. Many Type 2 glaciers in the Everest region have low-gradient tongues several kilometres in length, where base-level lakes could attain very large size. On Ngozumpa Glacier, for example, Spillway Lake could possibly expand up to 6 km upglacier, making it larger than any extant moraine-dammed lake in the region. The evolution of Ngozumpa Glacier – and other large Type 2 glaciers such as Khumbu Glacier – needs to be closely monitored in the coming years.

14. Future prospects

There have been some attempts to predict the future evolution of debris-covered glaciers in the Himalaya using numerical models, although to date these have been hampered by the lack of realistic mass balance functions or representations of lake-growth processes (e.g. Naito et al., 2000; Tangborn and Rana, 2000). The development and testing of such models, using the principles outlined in this paper, remain an important goal for the future.

Although much has been learned about the response of Himalayan debris-covered glaciers to climate change, considerable challenges still have to be met before fully quantitative predictive models can be applied. First, improved glacier mass balance modelling requires better coverage of meteorological data from high altitudes. Precipitation rates are especially poorly known, and are notoriously difficult to measure in high mountain regions. Important data could be obtained by systematic collection of snow/firn cores from accumulation basins, which integrate the effects of precipitation and redistribution processes such as wind-blow and avalanching, and also allow quantification of inter-annual variability. Second, there is a need for better parameterisation of ablation processes, including sub-debris melt and ice loss associated with the growth of supraglacial lakes. The complexity of Himalayan glacier surfaces, as well as the dependence of lake distribution on factors such as englacial structures, means that explicit modelling of the influence of supraglacial lakes on glacier ablation may remain impractical. However, it may be possible to approach the problem semi-empirically if correlations can be found between bulk ablation rates and easily measured factors such as perched lake area or glacier surface gradient. In addition, more data are required on the factors that control the growth of base-level lakes, especially subaqueous melting and calving.

GLOF hazards depend on a complex web of factors, including lake volume, dam characteristics and potential trigger mechanisms, and these may change through time. At-risk sites, therefore, need to be subject to continued monitoring, both in the field and using remote-sensing techniques. One such site is the terminal zone of Ngozumpa Glacier, where a base-level lake has recently entered a rapid growth phase (Thompson et al., 2012). Ngozumpa Glacier is stagnant for ~6.5 km upglacier of its terminus (Quincey et al., 2009), and the area available for lake growth suggests that lake volume could attain ~10^8 m^3 within the next 2 or 3 decades. This is one or two

orders of magnitude greater than extant moraine-dammed lakes in the region (Bajracharya and Mool, 2009).

Predictions of the impacts of reduced glacier volume are often highly contentious, and it can be hard to reconcile the need and demands of human society with the inevitable uncertainties at the frontier of scientific understanding. Poorly informed predictions of glacier mass loss and exaggerated assessments of the probability and risk of GLOFs can do great damage to scientific credibility in the eyes of local communities and the wider public (Watanabe et al., 2009; Cogley et al., 2010). It is therefore imperative that predictions of glacier response to climate change have a sound scientific basis, and that clear criteria are developed for prioritising mitigation efforts. Our understanding of how Himalayan glacier systems behave has increased greatly in recent years, but focused effort is still required to address remaining data gaps and to develop fully quantitative predictive models.

Acknowledgements

References

Ageta, Y., Higuchi, K., 1984. Estimation of mass balance components of a summer-accumulation type glacier in the Nepal Himalaya. Geografiska Annaler 66A, 249–255.

Alley, R.B., Dupont, T.K., Parizek, B.R., Anandakrishnan, S., 2005. Access of surface meltwater to beds of sub-freezing glaciers: preliminary insights. Annals of Glaciology 40, 8–14.

Andermann, C., Bonnet, S., Gloaguen, R., 2011. Evaluation of precipitation data sets along the Himalayan front. Geochemistry, Geophysics, Geosystems 12, Q07023. doi:10.1029/2011GC003513.

Asahi, K., 2010. Equilibrium-line altitudes of the present and Last Glacial Maximum in the eastern Nepal Himalayas and their implications for SW monsoon climate. Quaternary International 212, 26–34.

Bajracharya, S.R., Mool, P.K., 2009. Glaciers, glacial lakes and glacial lake outburst floods in the Mount Everest region, Nepal. Annals of Glaciology 50, 81–86.

Barros, A.P., Kim, G., Williams, E., Nesbitt, S.W., 2004. Probing orographic controls in the Himalayas during the monsoon using satellite imagery. Natural Hazards and Earth System Sciences 4, 29–51.

Barsch, D., Jakob, M., 1998. Mass transport by active rock glaciers in the Khumbu Himalaya. Geomorphology 26, 215–222.

Benn, D.I., Lehmkuhl, F., 2000. Mass balance and equilibrium-line altitudes of glaciers in high mountain environments. Quaternary International 65 (66), 15–29.

Benn, D.I., Owen, L.A., 2002. Himalayan glacial sedimentary environments: a framework for reconstructing and dating the former extent of glaciers in high mountains. Quaternary International 97–98, 3–25.

Benn, D.I., Wiseman, S., Warren, C.R., 2000. Rapid growth of a supraglacial lake, Ngozumpa Glacier, Khumbu Himal, Nepal. In: Nakawo, N., Fountain, A., Raymond, C. (Eds.), Debris-Covered Glaciers. IAHS Publications, pp. 177–185. 264.

Benn, D.I., Wiseman, S., Hands, K.A., 2001. Growth and drainage of supraglacial lakes on the debris-mantled Ngozumpa Glacier, Khumbu Himal, Nepal. Journal of Glaciology 47, 626–638.

Benn, D.I., Kirkbride, M.P., Owen, L.A., Brazier, V., 2003. Glaciated valley landsystems. In: Evans, D.J.A. (Ed.), Glacial Landsystems. Arnold, pp. 372–406.

Benn, D.I., Warren, C.R., Mottram, R.H., 2007. Calving processes and the dynamics of calving glaciers. Earth-Science Reviews 82, 143–179.

Benn, D.I., Gulley, J., Luckman, A., Adamek, A., Glowacki, P., 2009. Englacial drainage systems formed by hydrologically assisted fracture propagation. Journal of Glaciology 55 (191), 513–523.

Bertolani, L., Bollasina, M., Verza, G.P., Tartari, G., 2000. Pyramid Meterorological Station: Summary Report 1994–1998. Ev-K2-CNR Committee, Milan.

Bhatt, B.C., Nakamura, K., 2005. Characteristics of monsoonal rainfall around the Himalayas revealed by TRMM Precipitation Radar. Monthly Weather Review 133, 149–165.

Bolch, T., Buchroithner, M., Peters, J., Baessler, M., Bajracharya, S., 2008a. Identification of glacier motion and potentially dangerous glacial lakes in the Everest region/ Nepal using spaceborne imagery. Natural Hazards and Earth System Science 8, 1329–1340.

Bolch, T., Buchroithner, M., Pieczonka, T., Kunert, A., 2008b. Planimetric and volumetric glacier changes in the Khumbu Himal, Nepal, since 1962 using Corona, Landsat TM and ASTER data. Journal of Glaciology 54 (187), 592–600.

Bolch, T., Pieczonka, T., Benn, D.I., 2011a. Multi-decadal mass loss of glaciers in the Everest area (Nepal, Himalaya) derived from stereo imagery. The Cryosphere 5, 349–358.

Bookhagen, B., Burbank, D., 2006. Topography, relief, and TRMM-derived rainfall variations along the Himalaya. Geophysical Research Letters 33, L08405.

Buchroithner, M., Jentsch, G., Wanivenhaus, B., 1982. Monitoring of recent geological events in the Khumbu area (Himalaya, Nepal) by digital processing of Landsat MSS Data. Rock Mechanics 15, 181–197.

Casey, K.A., Kääb, A., Benn, D.I., 2012. Geochemical characterization of supraglacial debris via in situ and optical remote sensing methods: a case study in Khumbu Himalaya, Nepal. The Cryosphere 6, 85–100.

Chikita, K., Jha, J., Yamada, T., 1999. Hydrodynamics of a supraglacial lake and its effect on the basin expansion: Tsho Rolpa, Rolwaling Valley, Nepal Himalaya. Arctic, Antarctic, and Alpine Research 31, 58–70.

Chikita, K., Jha, J., Yamada, T., 2001. Sedimentary effects on the expansion of a Himalayan supraglacial lake. Global and Planetary Change 28, 23–34.

Clague, J.J., Evans, S.G., 2000. A review of catastrophic drainage of moraine-dammed lakes in British Columbia. Quaternary Science Reviews 19, 1763–1783.

Cogley, J.G., Kargel, J.S., Kaser, G., van der Veen, C.J., 2010. Tracking the source of glacier misinformation. Science 327, 522.

Fountain, A.G., Walder, J., 1998. Water flow through temperate glaciers. Reviews of Geophysics 36, 299–328.

Fujita, K., Nuimura, T., 2011. Spatially heterogeneous wastage of Himalayan glaciers. Proceedings of the National Academy of Sciences of the United States of America 108 (34), 14011–14014. doi:10.1073/pnas.1106242108.

Fujita, K., Kadota, T., Rana, B., Kayastha, R.B., Ageta, Y., 2001. Shrinkage of Glacier AX010 in Shorong region, Nepal Himalayas in the 1990s. Bulletin of Glaciological Research 18, 51–54.

Fujita, K., Sakai, A., Nuimura, T., Yamaguchi, S., Sharma, R.R., 2009. Recent changes in Imja glacial lake and its damming moraine in the Nepal Himalaya revealed by in situ surveys and multi-temporal ASTER imagery. Environmental Research Letters 4. doi:10.1088/1748-9326/4/4/045205.

Fukui, K., Fujii, Y., Ageta, Y., Asahi, K., 2007. Changes in the lower limit of mountain permafrost between 1973 and 2004 in the Khumbu Himal, the Nepal Himalayas. Global and Planetary Change 55, 251–256.

Fushimi, H., Yoshida, M., Watanabe, O., Upadhyay, B.P., 1980. Distributions and grain sizes of supraglacial debris in the Khumbu Glacier, Khumbu Region, East Nepal. Seppyo 42, 18–25.

Gades, A., Conway, H., Nereson, N., Naito, N., Kadota, T., 2000. Radio echo-sounding through supraglacial debris on Lirung and Khumbu Glaciers, Nepal Himalayas. In: Nakawo, N., Fountain, A., Raymond, C. (Eds.), Debris-Covered Glaciers: IAHS Publications, pp. 13–22. 264.

Gulley, J., Benn, D.I., 2007. Structural control of englacial drainage systems in Himalayan debris-covered glaciers. Journal of Glaciology 53, 399–412.

Gulley, J., Benn, D.I., Luckman, A., Müller, D., 2009a. A cut-and-closure origin for englacial conduits on uncrevassed parts of polythermal glaciers. Journal of Glaciology 55 (189), 66–80.

Gulley, J., Benn, D.I., Screaton, L., Martin, J., 2009b. Englacial conduit formation and implications for subglacial recharge. Quaternary Science Reviews 28 (19–20), 1984–1999.

Hambrey, M.J., Quincey, D.J., Glasser, N.F., Reynolds, J.M., Richardson, S.D., Clemmens, S., 2008. Sedimentological, geomorphological and dynamic context of debris-mantled glaciers, Mount Everest region, Nepal. Quaternary Science Reviews 27 (25–26), 2361–2389.

Hands, K. 2004. Downwasting and supraglacial pond evolution on the debris-mantled Ngozumpa glacier, Khumbu Himal, Nepal. Unpublished PhD thesis, University of St Andrews.

Higuchi, K., Fushimi, H., Ohata, T., Takenaka, S., Iwata, S., Yokoyama, K., Higuchi, H., Nagoshi, A., Iozawa, T., 1980. Glacier inventory in the Dudh Kosi region, East Nepal. IAHS-AISH Publications, 126, pp. 95–103.

Higuchi, K., Watanabe, O., Fushimi, H., Takenaka, S., Nagoshi, A., 2010. Glaciers of Nepal. In: Williams Jr., R.S., Ferrigno, J.G. (Eds.), Glaciers of Asia: U.S. Geological Survey Professional Paper 1386-F.

Huggel, C., Haeberli, W., Kääb, A., Bieri, D., Richardson, S., 2004. An assessment procedure for glacial hazards in the Swiss Alps. Canadian Geotechnical Journal 41, 1068–1083.

Iken, A., 1977. Movement of a large ice mass before breaking off. Journal of Glaciology 19, 595–604.

Inoue, J., Yoshida, M., 1980. Ablation and heat exchange over the Khumbu Glacier. Seppyo 41, 9–17 Special Issue.

Iwata, S., Aoki, T., Kadota, T., Seko, K., Yamaguchi, S., 2000. Morphological evolution of the debris cover on Khumbu Glacier, Nepal, between 1978 and 1995. In: Nakawo, N., Fountain, A., Raymond, C. (Eds.), Debris-Covered Glaciers: IAHS Publications, 264, pp. 3–11.

Jakob, M., 1992. Active rock glaciers and the lower limit of discontinuous alpine permafrost, Khumbu Himalaya, Nepal. Permafrost and Periglacial Processes 3, 253–256.

Jordan, R.E., Stark, J.A., 2001. Capillary tension in rotting ice layers. Technical Report ERDC/ CRREL TR-01-13. Cold Regions Research and Engineering Laboratory, New Hampshire. 15 pp.

Kadota, T., Fujita, K., Seko, K., Kayastha, R.B., Ageta, Y., 1997. Monitoring and prediction of shrinkage of a small glacier in the Nepal Himalaya. Annals of Glaciology 24, 90–94.

Kaspari, S., Mayewski, P., Kang, S., Sneed, S., Hou, S., Hooke, R. LeB, Kreutz, K., Introne, D., Handley, M., Maasch, K., Qin, D., Ren, J., 2007. Reduction in northward

incursions of the South Asian monsoon since 1400 AD inferred from a Mt. Everest ice core. Geophysical Research Letters 34, L16701. doi:10.1029/2007GL030440.

Kaspari, S., Hooke, R. LeB, Mayewski, P.A., 2008. Snow accumulation rate on Qomolongma (Mount Everest), Himalaya: synchroneity with sites across the Tibetan Plateau on 50–100 year timescales. Journal of Glaciology 54 (185), 343–352.

Kattelmann, R., 2003. Glacial lake outburst floods in the Nepal Himalaya: a manageable hazard? Natural Hazards 28, 145–154.

Kennett, E.J., Toumi, R., 2005. Himalayan rainfall and vorticity generation within the Indian summer monsoon. Geophysical Research Letters 32 (4), L04802.

Kirkbride, M.P., 1993. The temporal significance of transitions from melting to calving termini at glaciers in the central Southern Alps of New Zealand. The Holocene 3, 232–240.

Kirkbride, M.P., 2000. Ice marginal geomorphology and Holocene expansion of debris-covered Tasman Glacier, New Zealand. In: Nakawo, N., Fountain, A., Raymond, C. (Eds.), Debris-Covered Glaciers: IAHS Publications, 264, pp. 211–217.

Kirkbride, M.P., Warren, C.R., 1999. Tasman Glacier, New Zealand: 20th century thinning and predicted calving retreat. Global and Planetary Change 22, 11–28.

Kodama, H., Mae, S., 1976. Flow of glaciers in the Khumbu region. Seppyo Special Issue 30 (1), 31–36.

Komori, J., Gurung, D.R., Iwata, S., Yabuki, H., 2004. Variation and lake expansion of Chubda Glacier, Bhutan Himalayas, during the last 35 years. Bulletin of Glaciological Research 21, 49–55.

Lamsal, D., Sawagaki, T., Watanabe, T., 2011. Digital terrain modelling using Corona and ALOS PRISM data to investigate the distal part of Imja Glacier, Khumbu Himal, Nepal. Journal of Mountain Science 8, 390–402.

Luckman, A., Quincey, D.J., Bevan, S., 2007. The potential of satellite radar interferometry and feature tracking for monitoring flow rates of Himalayan glaciers. Remote Sensing of Environment 111, 172–181.

Mann, D.H., Sletten, R.S., Reanier, R.E., 1996. Quaternary glaciation of the Rongbuk valley, Tibet. Journal of Quaternary Science 11, 267–280.

Naito, N., Nakawo, M., Kadota, T., Raymond, C.R., 2000. Numerical simulation of recent shrinkage of Khumbu Glacier, Nepal Himalayas. In: Nakawo, N., Fountain, A., Raymond, C. (Eds.), Debris-covered Glaciers: IAHS Publications, 264, pp. 245–254.

Nakawo, M., Iwata, S., Watanabe, O., Yoshida, M., 1986. Processes which distribute supraglacial debris on the Khumbu Glacier, Nepal Himalaya. Annals of Glaciology 8, 129–131.

Nakawo, M., Yabuki, H., Sakai, A., 1999. Characteristics of Khumbu Glacier, Nepal Himalaya: recent changes in the debris-covered area. Annals of Glaciology 28, 118–122.

Nicholson, L., 2005. Modelling melt beneath supraglacial debris: implications for the climatic response of debris-covered glaciers. Unpublished PhD thesis, University of St. Andrews, UK.

Nicholson, L., Benn, D.I., 2006. Calculating ice melt beneath a debris layer using meteorological data. Journal of Glaciology 52 (178), 463–470.

Nuimura, T., Fujita, K., Fukui, K., Asahi, K., Aryal, R., Ageta, Y., 2011. Temporal changes in elevation of the debris-covered ablation area of Khumbu Glacier in the Nepal Himalaya since 1978. Arctic, Antarctic, and Alpine Research 43 (2), 246–255.

Osti, R., Bhattari, T.N., Miyake, K., 2011. Causes of catastrophic failure of Tam Pokhari moraine dam in the Mt. Everest region. Natural Hazards 58, 1209–1223.

Owen, L.A., Robinson, R., Benn, D.I., Finkel, R.C., Davis, N.K., Yi, C., Putkonen, J., Li, D., Murray, A.S., 2009. Quaternary glaciation of Mount Everest. Quaternary Science Reviews 28, 1412–1433.

Quincey, D.J., 2006. Remote sensing methods for high-mountain glacial hazard assessment. Unpublished PhD thesis, University of Wales, Aberystwyth, UK.

Quincey, D.J., Richardson, S.D., Luckman, A., Lucas, R.M., Reynolds, J.M., Hambrey, M.J., Glasser, N.F., 2007. Early recognition of glacial lake hazards in the Himalaya using remote sensing datasets. Global and Planetary Change 56, 137–152.

Quincey, D.J., Luckman, A., Benn, D.I., 2009. Quantification of Everest-region glacier velocities between 1992 and 2002, using satellite radar interferometry and feature tracking. Journal of Glaciology 55, 596–606.

Radić, V., Hock, R., 2011. Regionally differentiated contribution of mountain glaciers and ice caps to future sea-level rise. Nature Geoscience 4, 91–94.

Rana, B., Shrestha, A.B., Reynolds, J.M., Aryal, R., Pokhrel, A.P., Budhathoki, K.P., 2000. Hazard assessment of the Tsho Rolpa Glacier Lake and ongoing remediation measures. Journal of the Nepal Geological Society 22, 563–570.

Reid, T., Brock, B.W., 2010. An energy-balance model for debris-covered glaciers including heat conduction through the debris layer. Journal of Glaciology 56 (199), 903–916.

Reynolds, J.M., 1998. High-altitude glacial lake hazard assessment and mitigation: a Himalayan perspective. In: Maund, J.G., Eddleston, M. (Eds.), Geohazards in Engineering Geology: Geological Society, London, Engineering Geology Special Publications, 15, pp. 25–34.

Reynolds, J.M., 2000. On the formation of supraglacial lakes on debris-covered glaciers. In: Nakawo, N., Fountain, A., Raymond, C. (Eds.), Debris-covered Glaciers: IAHS Publications, 264, pp. 153–161.

Reynolds Geo-Sciences, 2003. Development of glacial hazard and risk minimization protocols in rural environments: guidelines for the management of glacial hazards and risks. Report No. R7816. 36 pp. (http://www.geologyuk.co.uk/mountain_hazards_group/dfid.htm).

Richards, B., Benn, D.I., Owen, L.A., Rhodes, E.J., Spencer, J.Q., 2000. Timing of late Quaternary glaciations south of Mount Everest in the Khumbu Himal, Nepal. Geological Society of America Bulletin 112, 1621–1632.

Richardson, S., Reynolds, J.M., 2000. Degradation of ice-cored moraine dams: implications for hazard development. In: Nakawo, N., Fountain, A., Raymond, C. (Eds.), Debris-covered Glaciers: IAHS Publications, 264, pp. 187–197.

Röhl, K., 2006a. Thermo-erosional notch development at fresh-water-calving Tasman Glacier, New Zealand. Journal of Glaciology 52 (177), 203–213.

Röhl, K., 2006b. Terminus disintegration of debris-covered, lake-calving glaciers. Unpublished PhD thesis, University of Otago, New Zealand.

Sakai, A., Fujita, K., 2010. Formation conditions of supraglacial lakes on debris-covered glaciers in the Himalaya (Letter). Journal of Glaciology 56 (195), 177–181.

Sakai, A., Nakawo, M., Fujita, K., 1998. Melt rate of ice cliffs on the Lirung Glacier, Nepal Himalayas, 1996. Bulletin of Glacier Research 16, 57–66.

Sakai, A., Takeuchi, N., Fujita, K., Nakawo, M., 2000a. Role of supraglacial ponds in the ablation process of a debris-covered glacier in the Nepal Himalaya. In: Nakawo, N., Fountain, A., Raymond, C. (Eds.), Debris-Covered Glaciers: IAHS Publications, 264, pp. 53–61.

Sakai, A., Chikita, K., Yamada, T., 2000b. Expansion of a moraine-dammed glacial lake, Tsho Rolpa, in Rolwaling Himal, Nepal Himalaya. Limnology and Oceanography 45, 1401–1408.

Sakai, A., Nakawo, M., Fujita, K., 2002. Distribution, characteristics and energy balance of ice cliffs on debris-covered glaciers, Nepal Himalaya. Arctic, Antarctic, and Alpine Research 34, 12–19.

Sakai, A., Nishimura, K., Kadota, T., Takeuchi, N., 2009. Onset of calving at supraglacial lakes on debris-covered glaciers of the Nepal Himalaya. Journal of Glaciology 55 (193), 909–917.

Scherler, D., Leprince, S., Stecker, M.R., 2008. Glacier-surface velocities in alpine terrain from optical satellite imagery — accuracy improvement and quality assessment. Remote Sensing of Environment 112, 3806–3819.

Scherler, D., Bookhagen, B., Strecker, M.R., 2011. Spatially variable response of Himalayan glaciers to climate change affected by debris cover. Nature Geoscience 4, 156–159.

Seko, K., Yabuki, H., Nakawo, M., Sakai, A., Kadota, T., Yamada, Y., 1998. Changing surface features of Khumbu Glacier, Nepal Himalayas, revealed by SPOT images. Bulletin of Glacier Research 16, 33–41.

Shrestha, A.B., Aryal, R., 2011. Climate change in Nepal and its impact on Himalayan glaciers. Regional Environmental Change. doi:10.1007/s10113-010-0174-9.

Shrestha, A.B., Wake, C.P., Mayewski, P.A., Dibb, J.E., 1999. Maximum temperature trends in the Himalaya and its vicinity: analysis based on temperature records from Nepal for the period 1971–94. Journal of Climate 12, 2775–2786.

Shrestha, A.B., Wake, C.P., Dibb, J.E., Mayewski, P.A., 2000. Precipitation fluctuations in the Nepal Himalaya and its vicinity and relationship with some large scale climatological parameters. International Journal of Climatology 20, 317–327.

Suzuki, R., Fujita, K., Ageta, Y., 2007. Spatial distribution of thermal properties on debris-covered glaciers in the Himalayas derived from ASTER data. Bulletin of Glaciological Research 24, 13–22.

Tangborn, W., Rana, B., 2000. Mass balance and runoff of the partially debris-covered Langtang Glacier, Nepal. In: Nakawo, N., Fountain, A., Raymond, C. (Eds.), Debris-Covered Glaciers: IAHS Publications, 264, pp. 99–108.

Thompson, S., Benn, D.I., Dennis, K., Luckman, A., 2012. A rapidly growing moraine-dammed glacial lake on Ngozumpa Glacier, Nepal. Geomorphology 75, 266–280.

Van der Veen, C.J., 1998. Fracture mechanics approach to penetration of surface crevasses on glaciers. Cold Regions Science and Technology 27 (1), 31–47.

Van der Veen, C.J., 2007. Fracture propagation as a means of rapidly transferring surface meltwater to the base of glaciers. Geophysical Research Letters 34 (1), L01501. http://dx.doi.org/10.1029/2006GL028385.

Vuichard, D., Zimmermann, M., 1987. The 1985 catastrophic drainage of a moraine-dammed lake, Khumbu Himal, Nepal: cause and consequences. Mountain Research and Development 7, 91–110.

Watanabe, O., Iwata, S., Fushimi, H., 1986. Topographic characteristics in the ablation area of the Khumbu Glacier, Nepal Himalaya. Annals of Glaciology 8, 177–180.

Watanabe, T., Lamsal, D., Ives, J.D., 2009. Evaluating the growth characteristics of a glacial lake and its degree of danger of outburst flooding: Imja Glacier, Khumbu Himal, Nepal. Norsk Geografisk Tidsskrift 63, 255–267.

Wessels, R.L., Kargel, J.S., Kieffer, H.H., 2002. ASTER measurement of supraglacial lakes in the Mount Everest region of the Himalaya. Annals of Glaciology 34, 399–408.

Wiseman, S., 2004. The inception and evolution of supraglacial lakes on debris-covered glaciers in the Nepal Himalaya. Unpublished PhD thesis, University of Aberdeen, UK.

Yamada, T., 1998. Glacier Lake and its Outburst Flood in the Nepal Himalaya. Monograph No. 1. Data Centre for Glacier Research, Japanese Society of Snow and Ice, Japan. 96 pp.

Yamada, T., Sharma, C.K., 1993. Glacier lakes and outburst floods in the Nepal Himalaya. Snow and Glacier Hydrology (Proceedings of the Kathmandu Symposium, November 1992): IAHS Publ., no. 218, pp. 319–330.

Yamamoto, M.K., Ueno, K., Nakamura, K., 2011. Comparison of satellite precipitation products with rain gauge data for the Khumbu Region, Nepal Himalayas. Journal of the Meteorological Society of Japan 89, 596–610.

Yang, X., Zhang, Y., Zhang, W., Yan, Y., Wang, Z., Ding, M., Chu, D., 2006. Climate change in Mt. Qomolangma region since 1971. Journal of Geographical Sciences 16, 326–336.

Yasunari, T., Inoue, J., 1978. Characteristics of monsoonal precipitation around peaks and ridges in Shorong and Khumbu Himal. Seppyo 40, 26–32 (Special Issue).